

# In vitro characterization of TNF-mediated programmed death in cells with optineurin deficiency

---

Dubaić, Karla

Master's thesis / Diplomski rad

2020

Degree Grantor / Ustanova koja je dodijelila akademski / stručni stupanj: **University of Rijeka / Sveučilište u Rijeci**

Permanent link / Trajna poveznica: <https://um.nsk.hr/um:nbn:hr:193:761888>

Rights / Prava: [In copyright](#) / [Zaštićeno autorskim pravom.](#)

Download date / Datum preuzimanja: **2024-09-20**

Repository / Repozitorij:



[Repository of the University of Rijeka, Faculty of Biotechnology and Drug Development - BIOTECHRI Repository](#)



UNIVERSITY OF RIJEKA  
DEPARTMENT OF BIOTECHNOLOGY  
Graduate program  
Biotechnology in Medicine

Karla Dubaić

*In vitro* characterization of TNF-mediated programmed death in cells with  
optineurin deficiency

Master's thesis

Rijeka, 2020

UNIVERSITY OF RIJEKA  
DEPARTMENT OF BIOTECHNOLOGY  
Graduate program  
Biotechnology in Medicine

Karla Dubaić

*In vitro* characterization of TNF-mediated programmed death in cells with  
optineurin deficiency

Master's thesis

Rijeka, 2020

Mentor: Ivana Munitić, MD, PhD

SVEUČILIŠTE U RIJECI  
ODJEL ZA BIOTEHNOLOGIJU  
Diplomski sveučilišni studij  
Biotehnologija u medicini

Karla Dubaić

In vitro karakterizacija TNF-om posredovane programirane stanične smrti  
u stanicama s deficijencijom optineurina

Diplomski rad

Rijeka, 2020

Mentor: izv. prof. dr. sc. Ivana Munitić

## **Acknowledgement**

*I wish to thank my mentor Ivana Munitić for her patient guidance, understanding and the knowledge I acquired throughout the months of this master thesis formation.*

*Special thanks to PhD student Nikolina Prtenjača and lab co-worker Valentina, who were always there to provide help and motivation when needed.*

*In the end, I want to thank my closest friends who were always there for me and my family who was always my biggest support.*

### Financial support

This work was supported by the Croatian Science Foundation grant IP-2018-01-8563), and the support of the University of Rijeka (18-211-1369) to dr.sc. Ivana Munitić. The equipment used for the study was financed by European Regional Development Fund (ERDF), within the project "Research Infrastructure for Campus-based Laboratories at University of Rijeka".

Master's thesis was defended on September 16, 2020

in front of the committee:

1. Associate Professor Rozi Andretić Waldowski
2. Assistant Professor Christian Reynolds
3. Associate Professor Ivana Munitić

The thesis has 42 pages, 11 figures, 47 references

## **Abstract**

In recent years neuroinflammation was found to be a major contributor to disease progression in neurodegenerative disorders such as amyotrophic lateral sclerosis (ALS). Inflammatory cytokines like tumor necrosis factor (TNF) can push cells into programmed cell death, such as apoptosis or necroptosis, which are mediated by receptor-interacting protein kinase 1 (RIPK1). It is not entirely clear what pushes cells to different forms of cell death. A recent study proposed that RIPK1 turnover is mediated by an adaptor protein optineurin, which is included in various cellular signaling and trafficking processes. Loss of optineurin was reported to be associated with enhanced motor neuron death and axonal degeneration, both of which are part of ALS pathology. However, this was not consistently reported in other studies, so the exact mechanism of action of optineurin in neuroprotection is still debated. Here, we focused on characterizing TNF-mediated programmed cell death in various optineurin-deficient cell lines. To address the role of optineurin in apoptosis and necroptosis, we first generated a novel mouse fibroblast (L929) optineurin knockout (Optn KO) cell line using CRISPR/Cas9 technique. L929 cells have been reported to be permissive to necroptotic cell death, so they were used to set up the assays. We induced necroptosis and apoptosis in wild-type (WT) and Optn KO L929 cells to determine the effect Optn KO on cell survival. Furthermore, we tested if cell types of the central nervous system (CNS), such as microglial (BV2) cells and neuronal (Neuro2A) cells, are dying by necroptosis. Our study confirmed that L929 cells are highly susceptible to necroptotic death. However, the survival rate of WT and Optn KO L929 cells was similar, which differs from previously published results. In BV2 and Neuro2A cells we detected a significant decrease in cell survival upon stimulating apoptosis and necroptosis, which was not rescued by caspase or RIPK1 inhibition. Notably, we did not detect any difference between WT and Optn KO BV2 cells, suggesting that optineurin deficiency does not sensitize microglia to TNF-mediated apoptosis and/or necroptosis. In

addition, our data suggest that another TNF-mediated mechanism may push cells to death, which is independent of caspases or RIPK1.

**Key words:** neuroinflammation, programmed cell death, optineurin, neurodegeneration



## Sažetak

Tijekom posljednjih godina je utvrđeno da neuroinflamacija snažno utječe na progresiju neurodegenerativnih bolesti poput amiotrofične lateralne skleroze (ALS). Upalni citokini poput faktora tumorske nekroze (TNF) mogu usmjeriti stanice u različite oblike stanične smrti uključujući apoptozu i nekroptozu, koje su posredovane protein-kinazom RIPK1 (prema engl. receptor-interacting protein kinase 1). Nije još u potpunosti razjašnjeno što tjera stanice u različite oblike smrti. Nedavna istraživanja predlažu da adaptorski protein optineurin, koji je uključen u niz signalnih i transportnih procesa u stanicama, regulira obrtaj RIPK1. Nedavno je objavljeno da je gubitak optineurina povezan s pojačanom smrću motorničkih neurona i aksonalnom degeneracijom, procesima koji su dio patologije ALS-a. Međutim, ti rezultati su opovrgnuti u nekoliko drugih studija i točan mehanizam optineurina u neuroprotekciji je još nejasan. U ovom radu, naglasak je stavljen na karakterizaciju TNF-om posredovane stanične smrti u različitim staničnim linijama u kojima je deletiran optineurin. Kako bismo analizirali ulogu optineurina u apoptozi i nekroptozu, prvo smo stvorili novu mišju fibroblastnu (L929) optineurin deficijentnu (Optn KO, prema engl. knockout) staničnu liniju pomoću CRISPR/Cas9 tehnologije. L929 stanice su sklone nekroptozu te su iz toga razloga korištene kao pozitivna kontrola. Potaknuli smo nekroptozu i apoptozu u stanicama divljeg tipa (WT) i Optn KO stanicama te promatrali preživljenje stanica. Osim toga, zanimalo nas je da li stanice bitne za središnji živčani sustav umiru nekroptozom, poput mikroglijalne (BV2) i WT neuronalne (Neuro2A) stanične linije. Potvrdili smo da su L929 stanice sklone nekroptotskoj smrti. Međutim, postotak preživljenja WT i Optn KO stanica bio je sličan, suprotno prije objavljenim rezultatima. U BV2 i Neuro2A stanicama smo primijetili značajno smanjeno preživljenje stanica nakon stimulacije apoptoze i nekroptoze, koje se nije poboljšalo nakon inhibicije kaspaza ili RIPK1. Značajno je da nismo otkrili razliku između WT i Optn KO BV2 stanica, što upućuje da deficijencija optineurina

ne senzibilizira mikrogliju prema TNF-om posredovanoj apoptozi i/ili nekroptozi. Štoviše, naši rezultati otvaraju mogućnost da postoji još jedan TNF-om posredovan mehanizam koji tjera stanice u smrt, neovisan o kaspazama ili RIPK1.

**Ključne riječi:** neuroinflamacija, programirana stanična smrt, optineurin, neurodegeneracija

# Contents

1. Introduction .....	1
1.1 Neuroinflammation in amyotrophic lateral sclerosis (ALS) pathogenesis .....	1
1.2 TNF mediated NF- $\kappa$ B activation .....	3
1.3. TNF-mediated cell death .....	6
1.3.1. Apoptosis .....	7
1.3.2. RIPK1-independent apoptosis (RIA) .....	8
1.3.3. RIPK1-dependent apoptosis (RDA).....	9
1.3.4. Necroptosis.....	10
1.4. The role of optineurin in cell death .....	12
2. Thesis goal.....	16
3. Materials and methods.....	17
3.1. Cell culture .....	17
3.2. Generation of Optn KO L929 cell line.....	17
3.3. Cell viability assay .....	18
3.4. Treatment for evaluating p-MLKL protein levels in L929 cell line ..	20
3.5. Protein analysis by Western blot .....	20
3.6. Statistical analysis .....	21
4. Results .....	22
4.1. Generation of Optn KO L929 cell line.....	22
4.2. No difference in necroptosis between L929 WT and Optn KO cells	23
4.3. MLKL is phosphorylated and degraded upon induction of nectoptosis in L929 cells .....	25
4.4. The extent and kinetics of MLKL phosphorylation is similar in WT and Optn KO L929 cells upon necroptosis induction .....	27
4.5. MLKL is not phosphorylated during apoptosis in L929 cell cells ....	28
4.6. WT and Optn KO BV2 cells are not sensitive to necroptosis or apoptosis .....	30
4.7. Neuro2A cells are not sensitive to necroptosis or apoptosis. ....	32
5. Discussion.....	34

6. Conclusion .....	38
7. References .....	39

# 1. Introduction

## 1.1 Neuroinflammation in amyotrophic lateral sclerosis pathogenesis

Amyotrophic lateral sclerosis (ALS) is a late-onset neurodegenerative disorder that primarily affects motor neurons in the motor cortex, brainstem and spinal cord <sup>1,2</sup>. Loss of neurons is a rapid process that leads to widespread paralysis and death within 3-5 years from the onset of symptoms <sup>3</sup>. Around 10% of ALS patients have a family history of ALS and are classified as familial (fALS) cases, while the remaining 90% of patients are sporadic with no apparent family history, classified as sporadic (sALS) cases <sup>2</sup>. However, this classification is vague, with newer research detecting genetic mutations in sALS cases, which arose either *de novo* or have previously been undetected in family members due to incomplete penetrance <sup>4</sup>. Notably, ALS is marked by large clinical and genetic heterogeneity <sup>2,5</sup>. Among >30 genes associated with ALS, pathogenic mutations in superoxide dismutase 1 (*SOD1*), chromosome 9 open reading frame 72 (*C9orf72*), TAR DNA-binding protein 43 (*TARDBP* or *TDP-43*) and fused in sarcoma (*FUS*) are most frequent, and account for most of the fALS cases in European population <sup>2</sup>. Other less frequent mutations include optineurin (*Optn*) and TANK-binding kinase (*TBK1*), two proteins that interact with each other, and could have a neuroprotective role <sup>2,5</sup>. All the above mentioned genes encode for proteins with rather distinct functions, and are thought to contribute to motor neuron injury through a wide range of processes including impaired proteostasis, impaired RNA metabolism, oxidative stress, cytoskeletal dysfunction, glutamate-mediated excitotoxicity, and mitochondrial dysfunction <sup>5,6</sup>. Impaired proteostasis is the most prominent hallmark of ALS. It results in accumulation of misfolded/aggregated proteins in neurons and glia. In most ALS cases, regardless of genetic background, inclusions usually contain an RNA-binding protein TDP-43. Although extensive research over the last couple of decades gained an insight into the complex genetic

background of ALS patients, it is still unclear how so many different processes lead to the same outcome and which mechanisms promote such rapid disease progression <sup>7</sup>.

An inflammatory response in the CNS, also known as neuroinflammation, is indirectly or directly linked to most of the above-mentioned ALS mutations <sup>1</sup>. Neuroinflammation is a common driving factor in other neurodegenerative disorders as well. In a healthy brain, neuroinflammation has an important role in protection against pathogens, promoting tissue repair by removing degenerating neurons, and enhancing synaptic plasticity <sup>8</sup>. This process is mediated through production of cytokines and chemokines by residential glial cells (microglia and astrocytes), and the surrounding endothelial cells <sup>8</sup>. The main coordinators of innate immune surveillance are microglia, a self-renewing population that makes up 5-15% of cells in the CNS parenchyma <sup>3</sup>. While constantly surveying their environment for potential threats (injury, pathogens), they are prepared for activation and cytokine production <sup>3</sup>. On their surface they express a large number of Toll-like receptors (TLRs) that recognize pathogen- and/or damage-associated molecular patterns (PAMPs and DAMPs), and pattern recognition receptors (PRRs) that bind foreign or misfolded proteins <sup>5,9</sup>. Upon receptor activation, microglia can assume two functionally different phenotypes: proinflammatory M1 phenotype also referred to as "classical activation" or immunosuppressive M2 phenotype that combines "alternative activation", and "acquired deactivation" <sup>10</sup>. When activated by a stimuli related to injury or infection, M1 microglia is the first line of defense in elimination of pathogens by producing proinflammatory cytokines such as tumor necrosis factor (TNF), interleukin-1-beta (IL-1 $\beta$ ), and other molecules like superoxide, nitric oxide (NO) and reactive oxygen species (ROS). Later in inflammation, microglia shifts to M2 state, marked by an increased production of IL-4 and IL-13 that promote anti-inflammatory responses, tissue repair and extracellular matrix reconstruction <sup>5,10</sup>. Acquired deactivation is also

crucial state in controlling microglial activation during acute inflammation, and is induced by production of IL-10 and transforming growth factor- $\beta$  (TGF- $\beta$ )<sup>10</sup>. Correct switch between the two states is necessary to control acute inflammation, in order to prevent excessive and/or chronic activation of microglia and potential damage of the surrounding tissue<sup>5</sup>.

It has been suggested that in neurodegenerative disorders, chronic inflammation is a primary cause of rapid disease progression<sup>1</sup>. Enhanced glial proliferation and activation, together with elevated proinflammatory cytokine levels were found in the blood and cerebrospinal fluid of ALS patients<sup>1,3,5</sup>. When microglia fail to deactivate, unregulated proinflammatory cytokine release promotes neuronal damage and death<sup>1</sup>. In this process there is a release of DAMPs, such as ALS-associated protein aggregates (TDP-43 and SOD1) and other common markers of cell death (HMGB1 and HSP-60) that bind to TLRs on microglia and activate them<sup>5,11</sup>. Moreover, through ROS production, microglia can directly harm surrounding neurons<sup>3</sup>. In ALS rodent models, presence of activated microglia around motor neurons is detected before any other symptoms, and stage of inflammation corresponds with disease progression. However, it is important to note that the presence of "activated" glia can contribute to both toxic and neuroprotective environments for neurons, so clearer understanding of neuronal-glia communication is necessary<sup>3</sup>.

## **1.2 TNF mediated NF- $\kappa$ B activation**

TNF was first described as a factor that leads to necrosis of transplantable tumors in mice, but now is broadly known as a proinflammatory cytokine accountable for the modulation of the immune response<sup>12,13</sup>. In the healthy CNS environment, basal activity of TNF has regulatory functions on synaptic plasticity, transmission and neuronal scaling in the brain cortex, striatum and hippocampus<sup>14</sup>. In pathological conditions when brain homeostasis is compromised, astrocytes and microglia release an

excessive amount of TNF, which contributes to chronic inflammation, glutamate-mediated cytotoxicity, synaptic loss and gliosis<sup>1,13</sup>. When TNF is released by the brain endothelial cells, neurons and residential glial cells, it leads to activation of NF- $\kappa$ B pathway. NF- $\kappa$ B is a transcription factor that regulates inflammation through proinflammatory cytokine production<sup>1</sup>. Various stimuli can activate this pathway, but in context of neurodegeneration most important are DAMPs and proinflammatory cytokines (TNF and IL-1) that promote signalosome assembly<sup>5</sup>.

TNF is first synthesized as a type II transmembrane protein (tmTNF), which then undergoes proteolytic cleavage within its extracellular domain by TNF converting enzyme (TACE) to form a soluble TNF homotrimer (sTNF). Both soluble and transmembrane TNF are biologically active and have distinct signal transduction pathways through two different surface receptors: TNF receptor 1 (TNFR1 or p55) and TNF receptor 2 (TNFR2 or p75). Each receptor has a specific binding affinity for TNF, downstream signaling cascade and biological functions<sup>12,13</sup>. Upon activation, TNFR1 promotes inflammatory responses and contributes to neuroinflammation and neurodegeneration, whereas some reports suggested that TNFR2 activation promotes anti-inflammatory responses and neuroprotection, thus promoting cell survival and tissue repair<sup>1,12</sup>. Moreover, TNFR1 is a death receptor (DR) and carries a death domain (DD) in the cytoplasm. DRs interact with cytoplasmic proteins containing DDs, which are essential for further signal transduction.

The binding of TNF to TNFR1 promotes the binding of TNFR1-associated death domain (TRADD) and RIPK1 to the receptor via their DD-DD interactions, and promotes formation of the TNFR1 complex I (Fig. 1). TRADD then further recruits TNFR-associated factor (TRAF2) and consequently cellular inhibitor of apoptosis protein 1 (cIAP1) and cIAP2, E3 ligases that normally form complexes with TRAF2 in cytoplasm<sup>15,16</sup>. cIAPs provide K63-polyubiquitylation and recruitment of linear ubiquitin



chain assembly complex (LUBAC). LUBAC comprises three proteins: haeme-oxidized IRP2 ubiquitin ligase 1 (HOIL1), HOIL1-interacting protein (HOIP) and SHANK-associated RH domain-interacting protein (SHARPIN), which then stabilize complex I with linear M1-linked polyubiquitin chains on RIPK1. Ubiquitin chains are essential for further recruitment and activation of signaling proteins: K63-polyubiquitylation, with higher affinity, provides a docking spot for transforming growth factor beta-activated kinase 1 (TAK1) and its adaptor protein TAK1-binding protein-2 (TAB2), while linear M1-linked polyubiquitin chains recruit I $\kappa$ B kinase (IKK) complex. IKK comprises three subunits: IKK $\alpha$ , IKK $\beta$  and NF- $\kappa$ B essential modulator (NEMO).

Upon phosphorylation by TAK1, IKK is activated and triggers the classical NF- $\kappa$ B pathway; phosphorylation and degradation of NF- $\kappa$ B inhibitor- $\alpha$  (I $\kappa$ B $\alpha$ ) and NF- $\kappa$ B release and translocation to nucleus. In nucleus, NF- $\kappa$ B activates transcription of genes important for cell survival, such as cellular FLICE-like inhibitory protein (cFLIP), proliferation and proinflammatory cytokine production<sup>1,15,16</sup>. cFLIP is an important apoptosis inhibitor that heterodimerizes with procaspase-8, thus preventing its activation<sup>16</sup>. To prevent hyperactivation of NF- $\kappa$ B signaling pathway, deubiquitylating enzymes (A20 and CYLD) deubiquitinate RIPK1 and stop further signaling<sup>15</sup>. NF- $\kappa$ B signaling pathway is important for regulation of immune response and in protecting cells against TNF-mediated death.

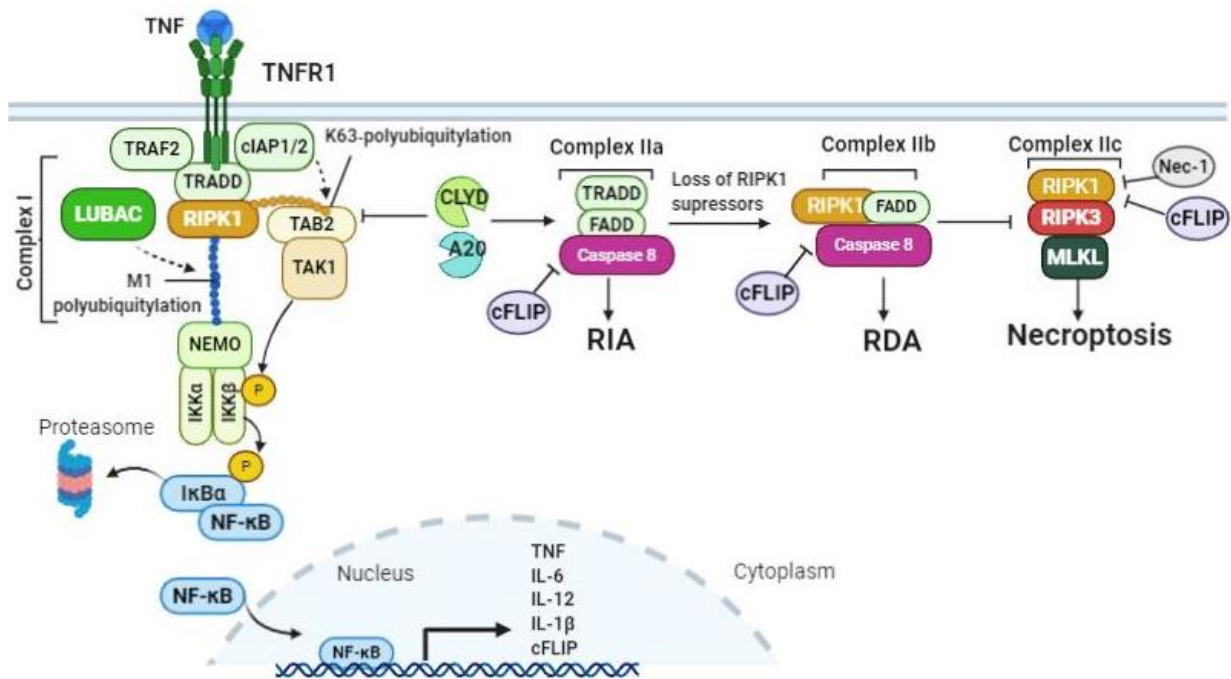


**Figure 1. TNF-mediated signaling pathways.** Upon TNF binding to TNFR1, formation of complex I begins. TRADD and RIPK1 bind to TNFR1 based on their DD-DD interactions. TRADD recruits TRAF2 and cIAP1/2, important for K63-polyubiquitylation and recruitment of LUBAC for M1- polyubiquitylation of RIPK1. **NF-κB signaling pathway:** M1-ubiquitin chains promote recruitment of IKKα, IKKβ and NEMO. TAK1 phosphorylates IKKβ, which then phosphorylates IκBα and releases NF-κB. NF-κB translocates to the nucleus and induces transcription of genes for cell survival and proinflammatory cytokine production. A20 and CYLD deubiquitylate RIPK1 and promote formation of death complexes. **RIPK1-independent apoptosis (RIA):** Complex IIa consists of TRADD, FADD and caspase-8 which then activates caspase-3 (not shown) and induces apoptosis. cFLIP negatively regulates apoptosis with caspase-8 inhibition. **RIPK1-dependent apoptosis (RDA):** Loss of suppressors of RIPK1 activation (cIAP1/2, LUBAC or kinases TAK1, TBK1 and IKK) promotes formation of complex IIb that consists of activated RIPK1, FADD and caspase-8. Caspase-8 activates caspase-3 (not shown) and induces apoptosis. **Necroptosis:** If caspases are inhibited, formation of complex IIc occurs that consists of RIPK1, RIPK3 and MLKL. RIPK1- RIPK3 interaction leads to RIPK3 autoactivation and phosphorylation of MLKL, resulting in cell lysis and necroptosis (not shown). cFLIP negatively regulates necroptosis through RIPK1 cleavage. Modified from: Yuan et al. 2019 <sup>17</sup>

### 1.3. TNF-mediated cell death

Considering the large amounts of TNF present in neuronal environment during neuroinflammation, it is reasonable to propose that some neurons undergo TNF-mediated cell death. When NF-κB pathway is inhibited, TNFR1 activation turns into a death signal <sup>18</sup>. TNFR1 activation has been

reported to promote several distinct types of cell death, including RIPK1-independent apoptosis (RIA), RIPK1-dependent apoptosis (RDA) and necroptosis<sup>19,20</sup>. These outcomes are highly regulated by two checkpoints during TNFR1 signaling: either by production of pro-survival/anti-apoptotic proteins through NF-κB pathway for blocking RIA or by inhibiting RIPK1 kinase activity for blocking RDA<sup>20</sup>.

### **1.3.1. Apoptosis**

Apoptosis is a form of regulated cell death, crucial for homeostasis and normal tissue development. First described in 1972, it is a best understood form of cell death described as mostly non-immunogenic with minimal damage to the surrounding microenvironment<sup>21,22</sup>. The induction of apoptosis depends on activation of different cysteine-aspartic proteases (caspases). Caspases are divided into two categories: initiator and executioner. The initiator caspases (caspase-8 and 9) get activated from their inactive form (procaspases) and activate the executioner procaspases (caspase-3, 6 and 7). Once activated, executioner caspases initiate characteristic morphological changes: cell blebbing and shrinkage, condensation of chromatin (pyknosis), nuclear fragmentation (karyorrhexis), and formation of small vesicles known as apoptotic bodies (ApoBDs). As a final step, ApoBDs or whole apoptotic cells are engulfed by residential phagocytes. Phagocytosis is a terminal step in apoptotic cycle and prevents discharge of cellular components into the surrounding tissue and damage to surrounding cells<sup>23</sup>.

There are two major apoptosis pathways, distinctive from each other based on the wide array of proteins and signal transducers involved: intrinsic and extrinsic<sup>23</sup>. The intrinsic apoptotic pathway can be induced by the cell itself upon damage detection through intracellular sensors which promote biochemical changes in the cell. This form of apoptosis is initiated either from positive or negative signals. Positive signals include exposure to hypoxia, radiation, ROS, toxins, viruses etc. Negative signals emerge in the absence of cytokines, growth factors and other pro-survival

signals<sup>21,23</sup>. When either of these triggers is present; apoptosis is induced, leading to disruption of mitochondrial transmembrane. Once membrane is obstructed, mitochondrial permeability transition (MPT) pore forms and makes membrane more permeable for pro-apoptotic proteins<sup>21</sup>. The extrinsic apoptosis pathway is receptor-mediated, through death receptors anchored to the cell membrane by their transmembrane regions. Once extracellular death ligands, produced by surveilling natural killer cells or macrophages, bind to death receptors, they transfer the signal into cytoplasm<sup>21,23</sup>. DRs belong to TNF receptor superfamily, and their activation depends on corresponding ligands: TNF and Fas<sup>21,23</sup>. Both TNF and Fas-mediated apoptotic pathway are similar and result in caspase-8 activation, which activates procaspase-3 in order to produce executor caspase-3. Executor caspase uses its preteolytic activity to cleave a variety of intracellular proteins and DNA<sup>16,23,24</sup>.

### **1.3.2. RIPK1-independent apoptosis (RIA)**

RIPK1 is a key kinase that regulates which TNF-mediated pathway cell will undertake, based on its ubiquitylation status<sup>19</sup>. Several deubiquitylating and ubiquitin-modifying enzymes can change the ubiquitylating status of RIPK1. A20 can remove K63-linked polyubiquitin chains (essential for LUBAC docking) and add K48-linked polyubiquitin chains to RIPK1, which pushes RIPK1 degradation and stops further signaling. CYLD is another deubiquitylating enzyme that removes K63- and M1-linked polyubiquitin chains (essential for IKK complex) from RIPK1. When RIPK1 is not ubiquitylated, pro-survival NF- $\kappa$ B signaling is turned off and RIPK1-containing complex dissociates from the membrane to form protein complexes that induce cell death (apoptosis or necroptosis)<sup>16</sup>.

Free and deubiquitylated RIPK1 helps to assemble complex IIa with TRADD, FADD and procaspase-8 in RIA (Fig. 1)<sup>16,19</sup>. Procaspase-8 then auto-cleaves itself to form active capase-8 that further activates executor caspase-3<sup>23</sup>. For studying RIA, NF- $\kappa$ B pathway must be inhibited. A

protein synthesis inhibitor cycloheximide (CHX) is commonly used for this purpose. CHX blocks the elongation phase during protein translation in eukaryotic cells, so during TNF-induced NF- $\kappa$ B signaling, synthesis of cFLIP and other pro-survival proteins is diminished<sup>20,25</sup> and cells are pushed to RIPK1-independent apoptosis.

### **1.3.3. RIPK1-dependent apoptosis (RDA)**

Unlike in RIA where kinase activity of RIPK1 is not needed, in RIPK1-dependent apoptosis the kinase activity of RIPK1 is necessary for the alternative complex IIb formation that consists of RIPK1, FADD and caspase-8 (Fig. 1)<sup>19,26</sup>. The exact cellular events that trigger cells to RDA are not entirely understood. This type of cell death is characterized with fast activation of RIPK1 in complex I and latter assembly of complex IIb that leads to apoptosis execution caspase-3<sup>20</sup>. RIPK1 activity regulation is highly complex web of ubiquitination and phosphorylation events that are recently discovered: TAK1 phosphorylates multiple residues on RIPK1 and suppresses its activity<sup>27</sup> as well as K63 ubiquitination of RIPK1 by cIAP1/2<sup>26,28</sup>. It is considered that failure of checkpoint mechanisms during TNFR1 signaling, such as loss of suppressors of RIPK1 activation (cIAP1/2, LUBAC or kinases TAK1, TBK1 and IKK), stimulates RDA<sup>26</sup>. To simulate RDA *in vitro*, commercially available agents that promote RDA are used, called SMAC mimetics. They are small molecules that mimic endogenous antagonists of cIAP1/2 and promote RIPK1 activation<sup>28</sup>. Also, CHX in combination with TNF was shown to promote RIPK1 activation and RDA when TAK1 phosphorylation of RIPK1 was blocked<sup>27</sup>.

Excessive pathologic cell death is connected to various neurodegenerative diseases<sup>21,26</sup>. In young CNS, intrinsic apoptosis has important role in forming a functional nervous system through proper neuron positioning and spacing, number reducing and neuroepithelial morphogenesis<sup>17,29</sup>. Adult neurons become rather resistant to intrinsic apoptosis, as possible adaptive mechanism to secure survival of neurons for decades. This resistance can be overcome in certain pathological conditions and

neurodegenerative diseases such as Parkinson disease (PD), Alzheimer disease (AD), multiple sclerosis (MS) and ALS, where extrinsic apoptosis pathway is activated and DRs are upregulated and contributing to further loss of neurons <sup>17</sup>.

#### **1.3.4. Necroptosis**

Contrary to apoptosis, necroptosis is a form of programmed cell death that is pro-inflammatory and caspase independent. It is characterized by organelle swelling, cytoplasmic granulation and finally cell membrane rupture that causes leakage of cellular content into the surrounding environment <sup>16,30</sup>. During cell lysis, release of DAMPs evokes inflammatory response from surrounding innate immune cells <sup>22</sup>. Necroptosis was first discovered in cell culture, when cells were stimulated with TNF in the presence of pan-caspase inhibitor z-VAD, a compound that blocks apoptosis in numerous cells types <sup>22,31</sup>. Cells were dying differently than from apoptosis, and the death itself required kinase activity of RIPK1. However, biological significance of this form of death was unknown until a subsequent study where cells infected with vaccinia virus (encoding for a viral caspase inhibitor) were dying from necroptosis. This suggested that necroptosis could be additional immune mechanism for battling viral infections <sup>22</sup>.

Most of the knowledge about necroptosis signaling comes from extensive studies using RIPK1 inhibitors (necrostatins, Nec-1) and animal models lacking proteins involved in complex IIc (also named necrosome) (Fig. 1), such as RIPK3 and MLKL through TNF-induced necroptotic pathway <sup>22,30</sup>. TNF with zVAD and CHX or SMAC mimetic, successfully induces necroptosis in different cell types <sup>22,27</sup>. As mentioned, upon TNFR1 activation cell has several options: NF-κB activation and cell survival, apoptosis or necroptosis. If cellular context and different cell death sensitizers are not pushing cell towards survival or apoptosis, the third option is necroptosis. When TNF binds to TNFR1, a complex I assembly

begins in same manner as in NF- $\kappa$ B and apoptosis. It is an essential platform for sequence of ubiquitylation and deubiquitylation events that dictate different outcomes. Caspase-8-FLIP heterodimers negatively control necroptosis through cleaving RIPK1. In condition where caspases or regulatory protein cFLIP are inhibited, with adequate amounts of RIPK3, MLKL and deubiquitylated RIPK1, necrosome is formed<sup>15,22,30</sup>. The necrosome complex contains RIPK1 and RIPK3, which interact via their RIP homotypic interaction motif (RHIM) domains. Oligomerization of RIPK3 leads to RIPK3 autoactivation and phosphorylation of MLKL (p-MLKL) following its translocation to the membrane<sup>15,30</sup>. In humans, MLKL phosphorylation at Thr357 and Ser358, causes conformational changes and oligomerization at the plasma membrane where it binds to phospholipids based on negative charge interactions<sup>22,30</sup>. Cell lysis occurs either through direct pore formation by MLKL oligomers, or indirectly by deregulating Ca<sub>2</sub><sup>+</sup> or Na<sup>+</sup> ion channels<sup>30</sup>. Phosphorylation of MLKL and its translocation to the membrane is a crucial step during necroptosis<sup>30</sup>. Therefore, detection of p-MLKL levels is a commonly used readout for necroptosis. Notably, antibodies against p-MLKL can be unspecific with additional band at 54 kDa<sup>27</sup>, so it is necessary to check antibody specificity before conducting further experiments.

The close interaction among inflammation and necroptosis supports the idea that necroptosis is linked to hyperinflammatory pathological conditions such as ALS<sup>3,30</sup>. In ALS patients, a common feature is pathological axonal 'Wallerian-like' degeneration characterized with axonal dystrophy or swelling, triggered by degeneration and dysfunction of oligodendrocytes<sup>17,32</sup>. In a specific mouse ALS model carrying the human SOD1<sup>G93A</sup> mutation, degeneration of oligodendrocytes and defects in axonal myelination were inhibited with RIPK1 inhibition and RIPK3 deficiency<sup>17</sup>. Several necroptotic markers including insoluble RIPK1, RIPK3, MLKL and p-MLKL were found elevated in post-mortem spinal cord samples of sALS patients. More direct link between necroptosis and motor

neuron death was discovered when astrocytes derived from sALS patients were co-cultured with motor neurons generated from human embryonic stem cells. Astrocytes derived from ALS patients, but not from the control, caused necroptotic motor neuron death; suggesting that surrounding environment dictates disease progression. Apart from SOD1, mutation causing haploinsufficiency of TBK1 is contributing to reduced expression of TAK1, an important RIPK1 suppressor. *Tbk1*<sup>+/-</sup> mice exhibited ALS symptoms, which were stopped upon RIPK1 inhibition<sup>17</sup>. These results indicate that reduced RIPK1 suppression facilitates necroptosis and neurodegeneration.

#### **1.4. The role of optineurin in cell death**

Optineurin is an adaptor protein involved in variety of cellular processes such as autophagy, Golgi maintenance, vesicular transport, signal transduction and inflammatory responses<sup>33,34</sup>. It is a highly conserved, ubiquitously expressed protein, with higher expression in heart, spleen, brain and skeletal muscle<sup>5,34</sup>. As an autophagy adaptor, optineurin interacts with TBK1, p62 and microtubule-associated proteins 1A/1B light chain 3B (LC3), proteins required in autophagy. With myosin VI, it forms a complex that enables protein trafficking and during inflammatory response, optineurin interacts with ubiquitinated RIPK1 and CYLD<sup>5,33,34</sup>. Possible explanation on why optineurin is involved in so many different processes is because of its direct/indirect interaction with various proteins, and some of them impact its function by adding post-translational modifications (phosphorylation and ubiquitination)<sup>33,34</sup>.

When optineurin protein structure was deciphered, several domains/interactions were found to be crucial for its function (Fig. 2). One of such is ubiquitin-binding domain (UBD), where K63 and M1 ubiquitylation provide signal transduction. Through UBD, optineurin binds with high affinity to myosin VI, RIPK1 and CYLD<sup>5,33,34</sup>.



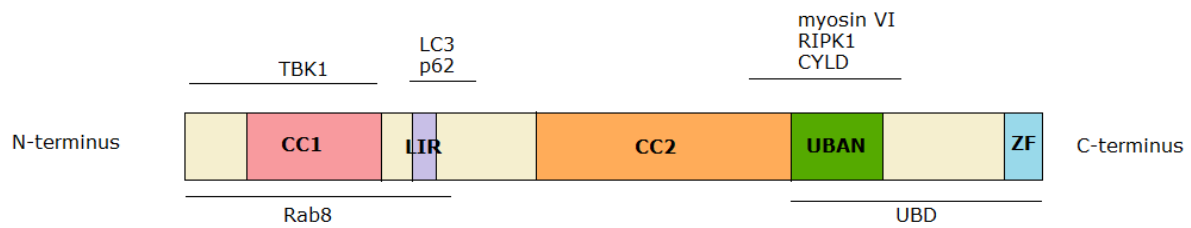


**Figure 2. The domains and interaction partners of optineurin.** N-terminus contains CC1: coiled-coil domain 1, LIR: LC3 interacting region, CC2: coiled-coil domain 2, UBAN: ubiquitin binding region of ABIN proteins and NEMO, and at the C-terminus is ZF: zinc finger. UBD domain of optineurin is important in context of this research for RIPK1 and CYLD binding.

Because of its high homology with NEMO, it was initially assumed that optineurin positively regulates the NF- $\kappa$ B pathway. This possibility was ruled out when in NEMO-deficient cells overexpressed optineurin did not activate NF- $\kappa$ B pathway<sup>35</sup>. Overexpression *in vitro* studies provided evidence that optineurin negatively regulates NF- $\kappa$ B pathway either through interaction with CYLD, or by binding to RIPK1 in the same manner as NEMO and precluding subsequent NF- $\kappa$ B activation<sup>5,36</sup>. Furthermore, silencing of optineurin in various cell lines induced higher NF- $\kappa$ B activity<sup>5</sup>. In contrast, results obtained from bone marrow-derived macrophages (BMDM) from *Optn*<sup>-/-</sup> or ubiquitin-binding deficient *Optn*<sup>D477N</sup> and *Optn*<sup>470T</sup> mice show normal, acute NF- $\kappa$ B activation<sup>5,33</sup>. Similar results were observed in primary microglia of *Optn*<sup>470T</sup> mice<sup>11</sup>. It is important to note that optineurin expression is regulated by the NF- $\kappa$ B pathway, so it is possible that optineurin regulates NF- $\kappa$ B activity, although this could depend on cell type, stimuli and type of inflammation (acute/chronic)<sup>5,34</sup>.

The first optineurin mutations connected to ALS were found in 2010 in Japanese patients and since then, more than 30 mutations were discovered that include deletions, missense and nonsense mutations<sup>33,34</sup>. Optineurin mutations have not been found to cause protein aggregates, unlike several other ALS mutations that are prone to aggregation and

toxicity due to gain-of-function, including SOD1, TDP-43 and FUS. Thus, it is thought that optineurin mutations act by: 1) loss-of-function, through deletions and nonsense mutations that encode for truncated protein or 2) they result in no protein at all. However, it is important to note that for the vast majority of optineurin mutations there is no adequate *in vitro/in vivo* model to study them, so the possibility remains that certain mutations can act by different pathogenic mechanism <sup>5</sup>.

Although it is known that optineurin mutations cause ALS, the mechanism is still unclear. Recent study with *Optn*<sup>-/-</sup> mice gained clearer insight into the neuroprotective role of optineurin. These mice had neuropathology that resembled ALS, including significantly lower number of motor axons, dysmyelination and Wallerian-like axonal pathology <sup>17,37</sup>. Moreover, spinal cord samples had elevated expression of TNF, RIPK1, RIPK3 and MLKL, biochemical hallmarks of necroptosis, which were reduced by RIPK1 inhibition <sup>17,37</sup>. Besides whole body *Optn* KO model, in order to determine the CNS cell types involved in ALS pathogenesis, they induced lineage-specific loss of optineurin in oligodendrocytes (using *Cnp-cre* mice), myeloid cell lineage (*Lyz2-cre* mice), astrocytes (*Gfap-cre* mice), motor neurons (*Mnx1-cre* mice) by treating *Optn*<sup>F/F</sup>;*Cx3cr1*<sup>Cre</sup> mice with tamoxifen for a month. Specific deletion of optineurin from myeloid cells, oligodendrocytes or microglia was enough to promote axonal myelination defects and degeneration similarly to what was observed in a whole body *Optn*<sup>-/-</sup> mice <sup>37</sup>. Coexpression analysis of primary *Optn*<sup>-/-</sup> microglia identified elevated LPS receptor CD14 and CD86, biomarkers for M1 active state, which were suppressed by *Nec-1s* and *Ripk1*<sup>D138N/D138N</sup> <sup>37</sup>. In this research, they hypothesized that RIPK1 activation stimulates proinflammatory state of *Optn*<sup>-/-</sup> microglia, not necroptosis. Surprisingly, one study from 2018, detected no myelin decompaction in *Optn*<sup>-/-</sup> mice and claims that such myelin decompaction is a result of myelin fixation, and it is not connected to disease progress <sup>38</sup>. Unlike in Ito et al. study, they found no change in spinal cord motor neuron number in one year old

Optn<sup>-/-</sup> mice. In addition, they found huge difference among *in vitro* and *in vivo* models. Constitutive deletion of RIPK3 in cultured mouse motor neurons protected them against toxicity of SOD1<sup>G93A</sup>-expressed astrocytes, while same RIPK3 loss in mice with additional SOD1<sup>G93A</sup> mutation showed no improvement on disease onset, motor neuron number, and survival *in vivo*. These results question if necroptosis has a detrimental role in ALS pathogenesis<sup>38</sup>.

## 2. Thesis goal

*In vivo* studies showed that optineurin-deficient mice exhibited ALS-like pathology with necroptosis and elevated levels of TNF, RIPK1, RIPK3 and MLKL, as reported in sporadic ALS patients as well. Research obtained on optineurin knockout L929 cells showed that they are highly sensitive to necroptosis<sup>37</sup>. This study also proposed a potential role of optineurin as a regulator of RIPK1 turnover. However, TNF-mediated programmed cell death in optineurin-deficient cells in the CNS has not been studied extensively, so its role in neurodegeneration is still debated. In addition, recent *in vivo* results showed that inhibition of necroptosis did not improve ALS pathology, questioning the role of necroptosis in motor neuron death<sup>38</sup>. To further analyze the role of optineurin in TNF-mediated cell death, we set the following goals in this thesis:

1. Establishing an optineurin knockout (Optn KO) mouse fibroblast (L929) cell line using CRISPR/Cas9 approach;
2. Setting up a cell survival experiment in wild-type (WT) and Optn KO L929 cells, and analyzing the difference in their susceptibility to apoptosis and/or necroptosis upon TNF stimulation;
3. Testing for necroptosis at the molecular level by assessing MLKL phosphorylation.
4. Comparing programmed cell death in WT and Optn KO microglial (BV2) cell lines, and analyzing programmed cell death in WT neuronal (Neuro2A) cell line.

### **3. Materials and methods**

#### **3.1. Cell culture**

Experiments were conducted on three different cell lines: immortalized wild-type (WT) murine microglia (BV2), neuroblastoma (Neuro2a), and murine fibroblasts (L929). Optineurin knockout (Optn KO) variants of Neuro2a and BV2 lines were previously generated by our group using CRISPR/Cas9 method <sup>6</sup>. BV2 and L929 cells were cultured in Dulbecco's Modified Eagle's Medium (DMEM, PAN Biotech), with supplementation of 10% fetal bovine serum (FBS), 1% L-glutamine and 1% of Penicillin/Streptomycin/Amphotericin B antibiotic mixture (PAN Biotech), henceforth labeled as complete DMEM. Neuro2a cells were cultured in Eagle's Minimal Essential Medium (EMEM, Pan Biotech), with supplementation of 10% FBS, 1% L-glutamine, 1% sodium pyruvate (PAN Biotech), 1% non-essential amino acids (PAN Biotech) and 1% Penicillin/Streptomycin/Amphotericin B antibiotic mixture, henceforth labeled as complete EMEM. For clonal selection, Optn KO variants were kept in medium enriched with puromycin (5 µg/mL for Neuro2A and 2 µg/mL for BV2). Cells were passaged every 2-3 days and incubated at 37°C and 5% CO<sub>2</sub>.

#### **3.2. Generation of Optn KO L929 cell line**

In order to generate L929 Optn KO cell line, original WT L929 cells were transfected with two lentiCRISPR v2 plasmids, each encoding for a guide RNA (gRNA)-sequence specific for optineurin together with Cas9 endonuclease and puromycin N-acetyl-transferase (a puromycin resistance protein). Transfection was achieved using Lipofectamine 3000 (Invitrogen), a reagent based on lipid nanoparticle technology, following the manufacturer's protocol. Following the previously established protocol <sup>6</sup> cells were seeded in the density of 100 000 and 200 000 cells/well on a 12-well plate in an antibiotic-free complete DMEM medium. For transfection of one well, 0.5 µg of each lentiCRISPR v2 plasmid was mixed

with 50  $\mu\text{L}$  of Opti-MEM medium (Gibco), 3  $\mu\text{L}$  of Lipofectamine 3000 and 2  $\mu\text{L}$  of P3000 Reagent. To determine the concentration of puromycin to be used for selection, different concentrations (10, 5, 2 and 1  $\mu\text{g}/\text{ml}$ ) were tested on non-transfected WT L929 cells. After 48h, concentration of 10  $\mu\text{g}/\text{ml}$  killed all non-transfected cells and was thus selected for generation of L929 Optn KO clones. Efficiency of CRISPR method and Optn deletion was confirmed by immunoblotting. Subsequently, the generated L929 Optn KO cell line was kept in puromycin enriched medium at 37°C and 5%  $\text{CO}_2$ .

### **3.3. Cell viability assay**

BV2, KO BV2, Neuro 2A, KO Neuro 2A, L929 and KO L929 cell lines were seeded at a density of 200 000 cells/well in 12 well plates. Cells were treated differently, in order to induce or inhibit apoptosis or necroptosis, as detailed below.

#### 1) Treatment for inducing and inhibiting necroptosis:

To induce necroptosis, we used TNF (10 ng/ml), CHX (0.5  $\mu\text{g}/\text{ml}$ ) and zVAD (20  $\mu\text{M}$ ). Before applying TNF and CHX, 30 min pre-incubation with zVAD (pan caspase inhibitor, Enzo) was done in order to push cells towards necroptotic cell death. In order to inhibit necroptosis, we added Nec-1 (50  $\mu\text{M}$ , RIPK1 inhibitor, Sigma) to cells treated with TNF, CHX, and zVAD. Nec-1 was pre-incubated in the same manner as zVAD. Control samples were treated with 4  $\mu\text{L}$  of DMSO.

#### 2) Treatment for inducing apoptosis and inhibiting RIPK1 dependent apoptosis

To induce apoptosis, we used TNF (10 ng/ml) and CHX (0.5  $\mu\text{g}/\text{ml}$ ). In order to inhibit RIPK1 dependent apoptosis, the same treatment remained with 30 min pre-incubation with Nec-1 (50  $\mu\text{M}$ ). Control samples were treated with 4  $\mu\text{L}$  of DMSO.

<b>WT (CTRL)</b> + 4 µl DMSO	<b>WT</b> CHX (0.5µg /ml)	<b>KO (CTRL)</b> + 4 µl DMSO	<b>KO</b> CHX (0.5µg /ml)
<b>WT</b> TNF (10 ng/ml ) CHX (0.5µg /ml)	<b>WT</b> TNF (10 ng/ml ) CHX (0.5µg /ml)	<b>KO</b> TNF (10 ng/ml ) CHX ( 0,5 µg /ml)	<b>KO</b> TNF (10 ng/ml ) CHX (0.5µg /ml)
<b>WT</b> TNF (10 ng/ml ) CHX (0.5µg /ml) zVAD (20 µM)	<b>WT</b> TNFa (10 ng/ml) CHX (0.5µg /ml) zVAD (20 µM)	<b>KO</b> TNFa (10 ng/ml) CHX (0.5µg /ml) zVAD (20 µM)	<b>KO</b> TNFa (10 ng/ml) CHX (0.5µg /ml) zVAD (20 µM)

**Figure 3. Treatment for inducing necroptosis and apoptosis**

<b>WT (CTRL)</b> + 4 µl DMSO		<b>KO (CTRL)</b> + 4 µl DMSO	
<b>WT</b> TNF (10 ng/ml ) CHX (0.5µg /ml) Nec - 1	<b>WT</b> TNF (10 ng/ml ) CHX (0.5µg /ml) Nec - 1	<b>KO</b> TNF (10 ng/ml ) CHX (0.5µg /ml) Nec - 1	<b>KO</b> TNF (10 ng/ml ) CHX (0.5µg /ml) Nec - 1
<b>WT</b> TNFa (10 ng/ml) zVAD (20 µM) CHX (0.5µg /ml) Nec - 1	<b>WT</b> TNFa (10 ng/ml) zVAD (20 µM) CHX (0.5µg /ml) Nec - 1	<b>KO</b> TNFa (10 ng/ml) zVAD (20 µM) CHX (0.5µg /ml) Nec - 1	<b>KO</b> TNFa (10 ng/ml) zVAD (20 µM) CHX (0.5µg /ml) Nec - 1

**Figure 4.: Treatment for blocking necroptosis and RIPK1 dependent apoptosis**

Twenty-four hours after treatment, all cells were collected and stained with Trypan blue. Number of live cells was established by counting on a Neubauer hemocytometer under Axio Vert.A1 (Zeiss) light microscope, using the following formula:

$$N(\text{cells})/\text{mL} = \frac{N (\text{total number of counted cells}) \times 10^4 (\text{square volume}) \times \text{dilution}}{n (\text{number of squares})}$$

### **3.4. Treatment for evaluating p-MLKL protein levels in L929 cell line**

To determine p-MLKL levels after inducing and blocking necroptosis, L929 WT and KO cells were seeded on a 12-well plate at a density of 200 000 cells/well. The following day, treatment with TNF (10 ng/ml), CHX (0.5 µg/ml), zVAD (20 µM) and necroptosis inhibitor Nec-1 (50 µM) was applied for 2, 4 or 6 h. Both z-VAD and Nec-1 were pre-incubated 30 min and controls were treated with 4 µL of DMSO.

### **3.5. Protein analysis by Western blot**

Proteins for Western blot analysis were obtained by washing cells with ice-cold PBS. The cells were subsequently lysed using ice-cold RIPA buffer (50 mM Tris, 150 mM NaCl, 0.5% sodium deoxycholate, 1% Triton X-100 (Fischer Scientific); pH 8) supplemented with protease and phosphatase inhibitors (Roche). Samples were transferred to 1.5 mL Eppendorf tubes, incubated on ice for 30 min, and centrifuged at + 4°C on 14 000 rpm for 10 min. Supernatants containing proteins were removed from the pellets and transferred to new 1.5 mL Eppendorf tubes and mixed in 3:1 ratio with 4X Laemmli sample buffer (50 mM Tris-HCl (pH 6.8), 10% glycerol, 2% SDS, 2% 2-mercaptoethanol, 0.04% bromophenol blue). For protein separation with sodium dodecyl sulfate-polyacrylamide gel electrophoresis (SDS-PAGE), 10% running gel (Milli-Q H<sub>2</sub>O, 0.375 M Tris (pH 8.8), 0.1% SDS, 10% acrylamide + bisacrylamide (Rotiphorese Gel 40), 0.1% ammonium persulfate (APS), 0.01% tetramethylethylenediamine (TEMED, Roth) and 6% stacking gel (6% acrylamide + bisacrylamide, 0.125 M Tris HCl (pH 6.8), 0.1 % SDS, 0.1 % APS, 0.01% TEMED) were used. Samples were heated for 10 min at 95°C, and loaded together with Tricolor Protein Marker (Roth). Electrophoresis was run on 100V for the first 30 min and



then on 130V for another hour. After electrophoresis, separated proteins were transferred from gel to nitrocellulose membrane (0.45  $\mu$ m pore, Invitrogen) for 80 min on 100 V. Nitrocellulose membrane was blocked for 1h in 5% BSA/TBST (Tris buffer saline (TBS; pH 7.4), 5% bovine serum albumin, 0.1% Tween 20) on a laboratory shaker, followed by primary antibody incubation overnight at + 4°C. Primary antibodies used were rabbit phospho-MLKL (p-MLKL; 1:1000 dilution; Cell Signaling Technologies), optineurin (1:1000 dilution; Cayman) and mouse MLKL (1:1000 dilution, Sigma). Following day, incubated membranes were washed 3x for 10 min in 0.1% TBS-T (TBS (pH 7.4), 0.1% Tween 20), incubated with secondary HRP-conjugated anti-rabbit antibody (1:2500, Jackson) for p-MLKL and anti-mouse antibody (1:400, Invitrogen) for MLKL, at room temperature (RT) for 1h. Primary rabbit antibody for  $\beta$ -actin (loading control) was already conjugated to HRP (1:2500; Sigma). Primary HRP conjugated rabbit  $\beta$ -actin was incubated 30 min at RT. All membranes were washed 3 times in 0.1% TBS-T prior to detection. Protein bands were visualized using chemiluminescent substrate (Lumi-light Western Blotting reagents, Roche), following manufacturer's protocol, on ChemiDoc MP (Bio-Rad). Results were quantified using Image J tool.

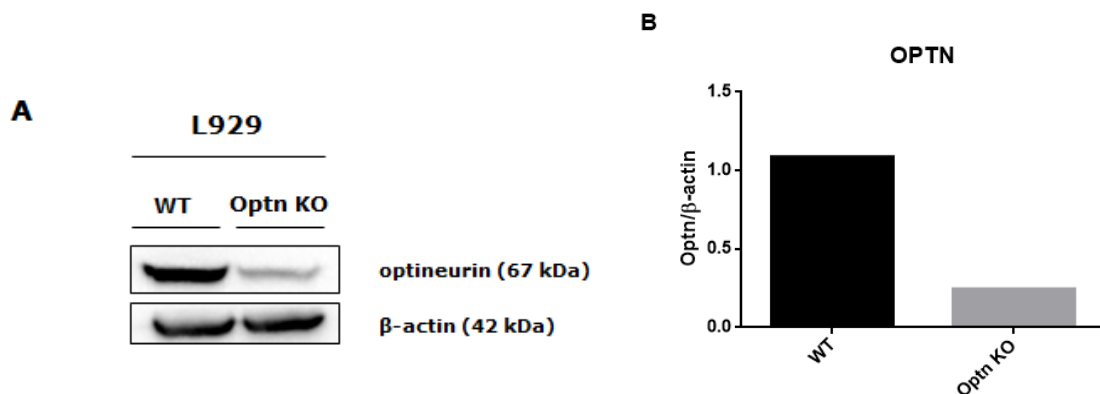
### **3.6. Statistical analysis**

Data shown represent means of independent experiments (indicated below figures). Statistical significance was determined using ordinary one-way ANOVA (GraphPad Prism) followed by Tukey's multiple comparisons post hoc test for pair-wise comparison. The value  $p < 0.05$  was considered statistically significant.

## 4. Results

### 4.1. Generation of Optn KO L929 cell line

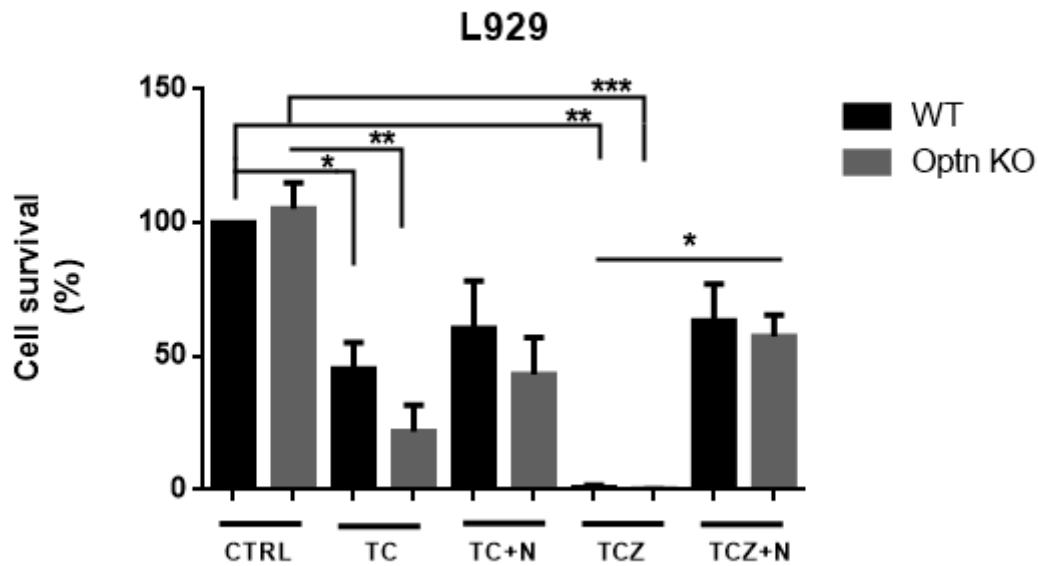
Not all cells are susceptible to necroptosis so for our initial experiments, we used L929 cell line, which undergoes TNF-mediated necroptosis when apoptosis is blocked<sup>18</sup>. To analyze the importance of optineurin for necroptosis, we generated Optn KO L929 cells. We used CRISPR/Cas9 approach, transfecting WT L929 cells with two lentiCRISPR v2 plasmids (this is in detail described in Materials and methods). Two weeks after the transfection and puromycin selection, clones were expanded and optineurin levels were assayed by immunoblotting. We confirmed that optineurin deletion in L929 cell line was largely successful, having detected a decrease of optineurin levels of over 80% (Fig.).



**Figure 5. Generation of Optn KO L929 cell line.** (A) Optineurin deletion was confirmed by western blotting using Optn antibody.  $\beta$ -actin was used as loading control. (B) Optineurin levels were quantified using ImageJ and normalized to  $\beta$ -actin. This experiment was conducted once so statistical significance could not be obtained.

## **4.2. No difference in necroptosis between L929 WT and Optn KO cells**

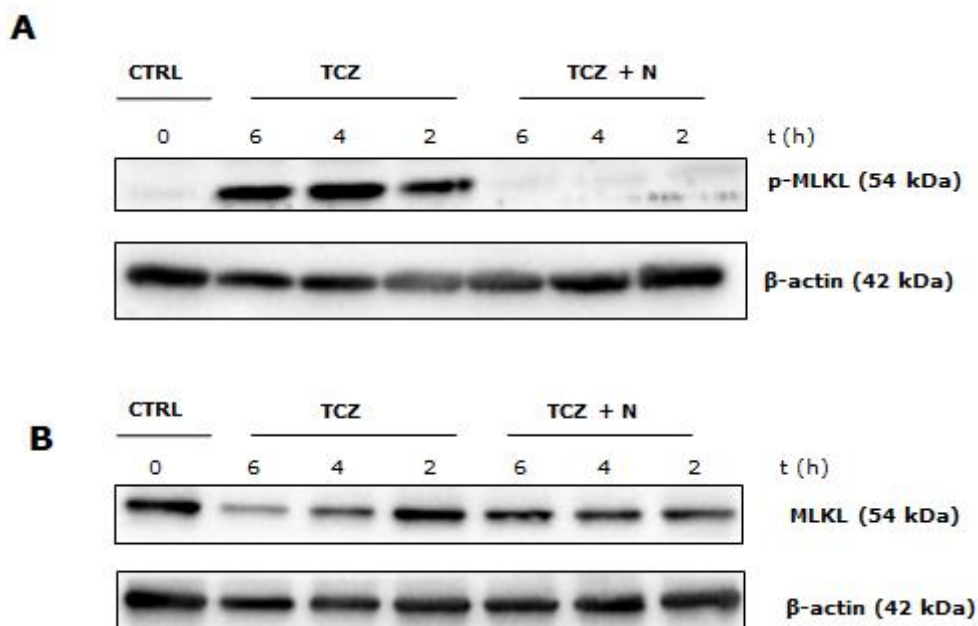
Once we generated Optn KO L929 cell line, we induced necroptosis and apoptosis in WT and Optn KO L929 cells. We plated cells in duplicates and at the same density and treated them with TNF (10 ng/ml) and CHX (0.5 µg/ml) to induce apoptosis through TNFR1 signaling pathway. To induce necroptosis, we pretreated cells with zVAD (20 µM) prior to adding TNF and CHX (in detail described in Materials and methods; this experimental condition is hereafter designed as TCZ). As a test for efficiency of necroptosis and RIPK1-dependent apoptosis, we used a RIPK1 inhibitor Nec-1 (50 µM). Twenty-four hours later, we collected and counted cells under the light microscope. The number of live cells after necroptosis treatment (TCZ) was significantly decreased, with only few viable cells left to count (Figure). This confirmed previous findings that L929 cells are highly susceptible to necroptosis<sup>18</sup>. When we used RIPK1 inhibitor, cell viability was 50% higher which confirms that L929 cells were dying from necroptosis. There was a statistically significant decrease in cell number after apoptosis (TC) treatment with an increase after RIPK1 inhibition, although it was not statistically significant. Furthermore, there was a tendency for Optn KO L929 cells to exhibit lower cell survival than WT L929 cells, but these findings would require additional confirmation. These results confirmed that L929 cells were dying from necroptosis but whether they were dying from RIA or RDA we could not distinguish. Moreover, Optn deficiency had a tendency to sensitize cells to apoptotic death, yet this was not statistically significant.



**Figure 6. No difference in cell survival between L929 WT and Optn KO cells upon necroptosis induction.** L929 WT and Optn KO cells were treated with TNF (10 ng/ml), CHX (0.5  $\mu$ g/ml), zVAD (20  $\mu$ M) for apoptosis (TC) or necroptosis (TCZ) with addition of RIPK1 inhibitor Nec -1 (50  $\mu$ M) (N) as indicated. Controls were treated with DMSO. Cell viability was assayed 24h upon treatment. Optn KO samples were normalized to WT counterparts from each experiment. Data are shown as mean  $\pm$  SEM of duplicate samples from two independent experiments (ordinary one-way ANOVA, followed by Tukey's multiple comparisons post hoc test for pair-wise comparison, \* $p$ <0.05, \*\* $p$ <0.01, \*\*\* $p$ <0.001).

### 4.3. MLKL is phosphorylated and degraded upon induction of nectoptosis in L929 cells

After the initial cell viability test, we wanted to measure phosphorylation of MLKL, a commonly used readout for necroptosis confirmation. To this end, we used WT cells and tested p-MLKL and MLKL antibody specificity. We seeded cells at density of 200 000 cells/well and treated them with TNF (10 ng/ml), CHX (0.5  $\mu$ g/ml), zVAD (20  $\mu$ M) and Nec-1 (50  $\mu$ M) for 2, 4 and 6 h, as described in the previous chapter. Western blot analysis showed an increase of p-MLKL as early as 2 h upon treatment with no MLKL degradation (Fig A and B). After 4 h, phosphorylation of MLKL reached its peak with consequent MLKL degradation (Fig B). At the 6 h time point phosphorylation began to reduce, possibly because more than 50 % of MLKL was degraded (Fig B). With addition of RIPK1 inhibitor, MLKL phosphorylation was suppressed at all time points and MLKL levels restored only at 6 h point (Fig A and B). Taken together, it emerged that MLKL degradation and phosphorylation occurred rapidly only 2 h after TNFR1 activation with further enhancement with time. RIPK1 inhibition confirmed TNF induced necroptosis in L929 cell line.



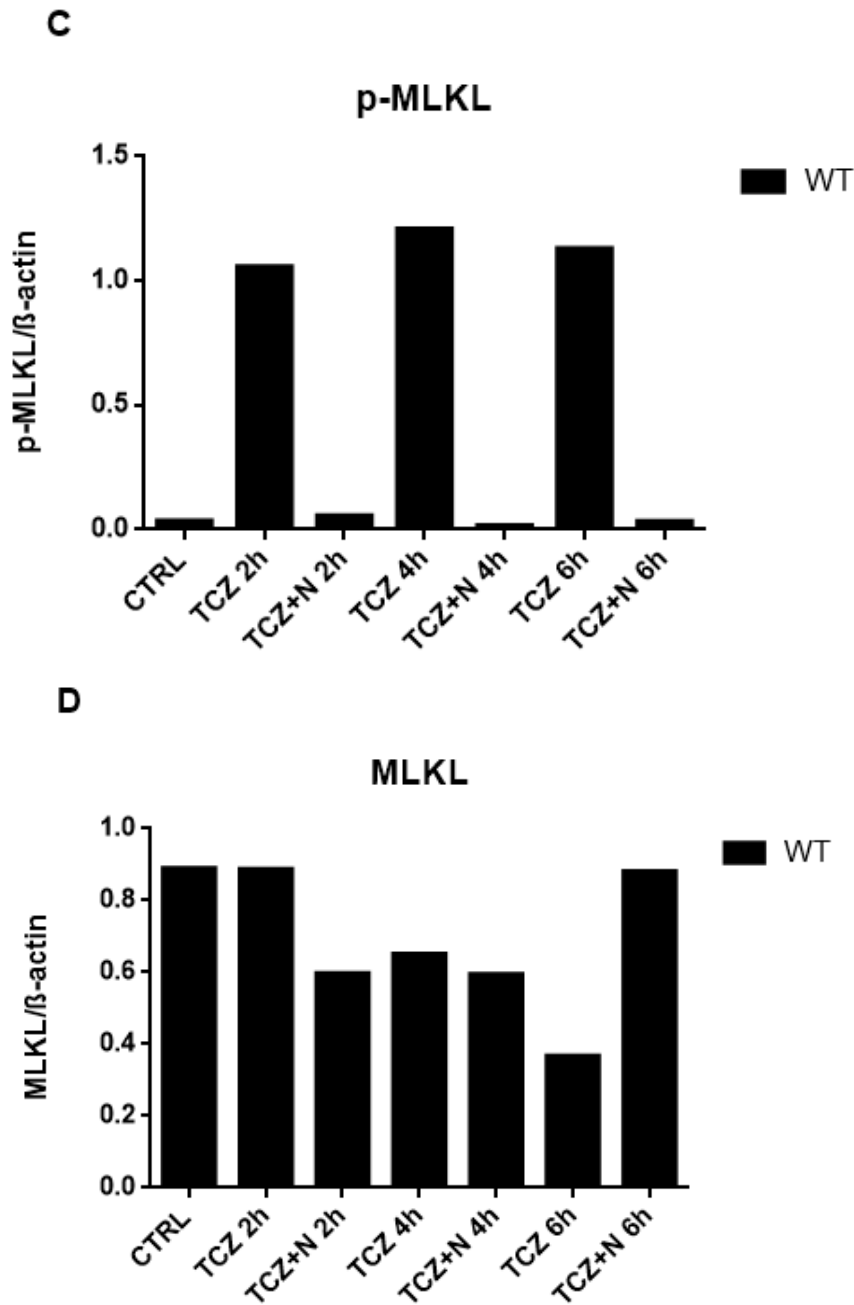
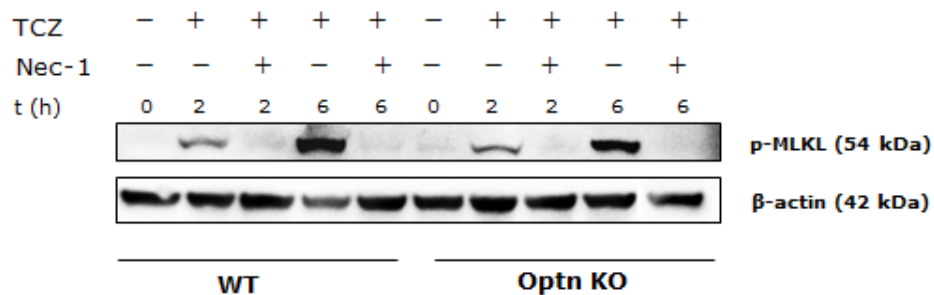


**Figure 7. MLKL gets phosphorylated and degraded upon induction of nectoptosis in L929 cells.** A) L929 WT cells were treated with TNF (10 ng/ml), CHX (0.5  $\mu$ g/ml), zVAD (20  $\mu$ M) (TCZ) with addition of RIPK1 inhibitor Nec -1 (50  $\mu$ M) (N) at the indicated time points. Controls were treated with DMSO for 6h. p-MLKL levels were detected by immunoblotting and  $\beta$ -actin was used as a loading control. (B) L929 WT cells were treated with TNF (10 ng/ml), CHX (0.5  $\mu$ g/ml), zVAD (20  $\mu$ M) (TCZ) with addition of RIPK1 inhibitor Nec -1 (50  $\mu$ M) (N) at the indicated time points. Controls were treated with DMSO for 6h. MLKL levels were detected by immunoblotting and  $\beta$ -actin was used as a loading control. (C) Densitometric quantification of p-MLKL is shown for the indicated time points. (D) Densitometric quantification of MLKL is shown for the indicated time points. The experiment was performed once so the statistical analysis could not be done.

#### 4.4. The extent and kinetics of MLKL phosphorylation is similar in WT and Optn KO L929 cells upon necroptosis induction

To test if optineurin deficiency sensitizes L929 cells to necroptotic death as previously shown <sup>37</sup>, we treated both WT and Optn KO L929 cells with previous treatment: TNF (10 ng/ml), CHX (0.5 µg/ml), zVAD (20 µM) and Nec-1 (50 µM) at selected time points of 2 and 6 h. After 2 h, the p-MLKL levels were elevated similarly in WT and Optn KO cells (Fig B). Upon 6 h treatment p-MLKL levels were twice as much than after 2 h, which confirmed that phosphorylation increased with time. There was visible difference between WT and Optn KO p-MLKL levels at 6 h after quantification; however that was not statistically significant (Fig B). L929 WT and Optn KO cells both expressed similar phosphorylation pattern after TNF-induced necroptosis, but optineurin deficiency did not sensitize cells to necroptosis based on obtained p-MLKL levels.

**A**



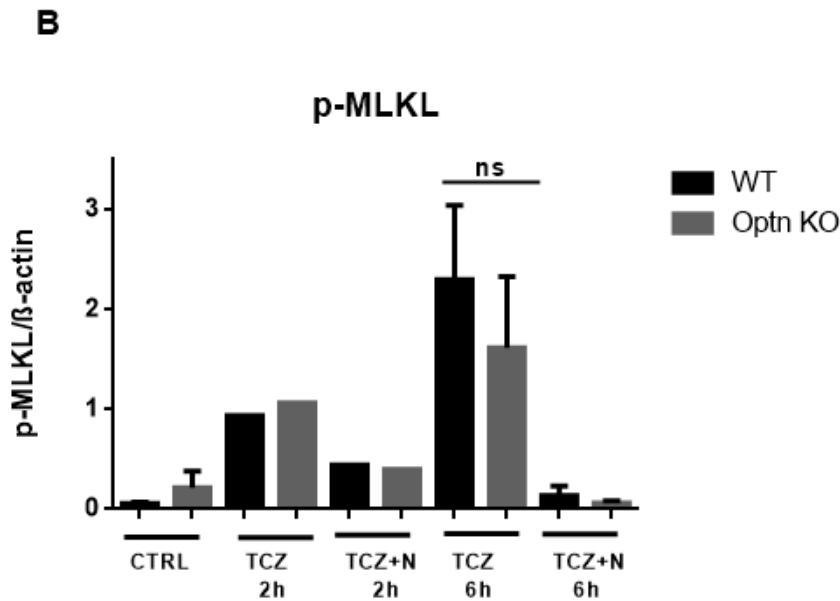


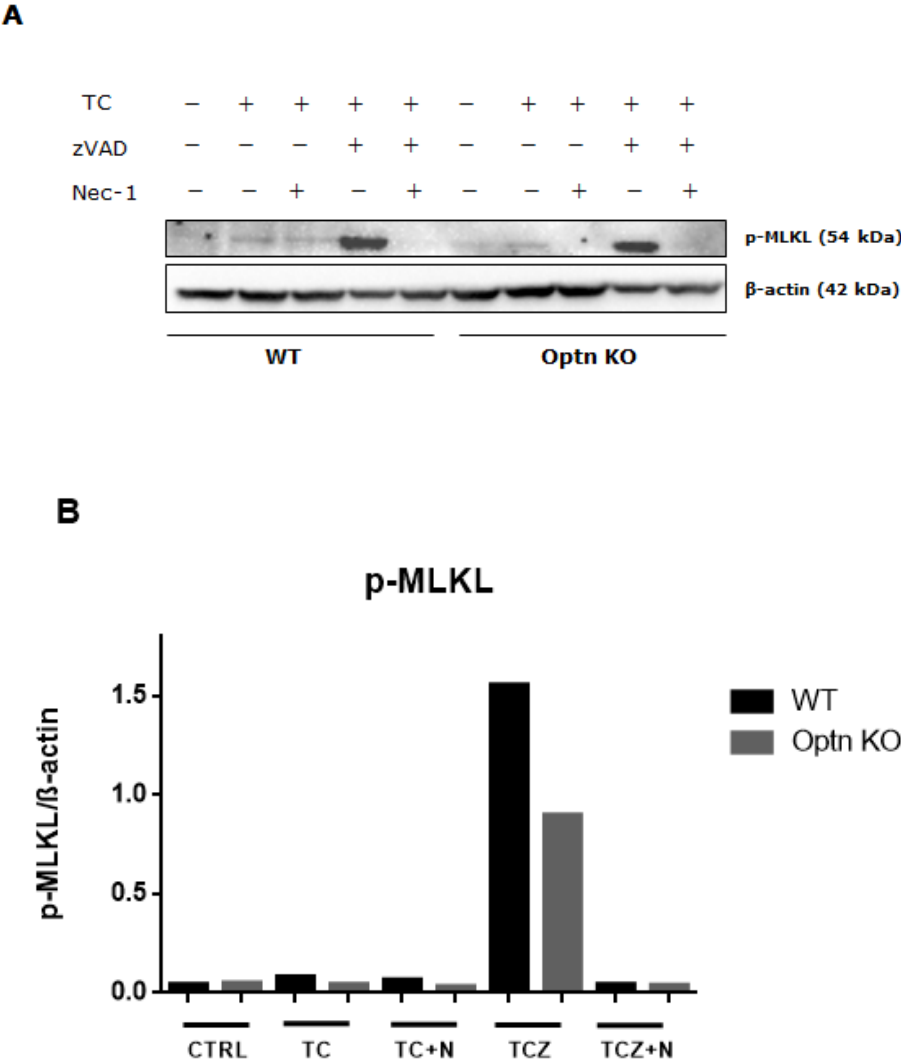
**Figure 8. Upon necroptosis induction MLKL is similarly phosphorylated in WT and Optn KO L929 cells.** (A) L929 WT and Optn KO cells were treated with TNF(10 ng/ml), CHX (0.5  $\mu$ g/ml), zVAD (20  $\mu$ M) (TCZ) with addition of RIPK1 inhibitor Nec -1 (50  $\mu$ M) (N) at indicated time points. Controls were treated with DMSO for 6h. p-MLKL was detected by immunoblotting, and  $\beta$ -actin was used as a loading control. (B) Densitometric quantification of p-MLKL at indicated time points. Data are shown as relative protein levels of one experiment for 2h treatment and as mean  $\pm$  SEM of two experiments for 6h treatment and control (ordinary one-way ANOVA, followed by Tukey's multiple comparisons post hoc test for pair-wise comparison, \* $p$ <0.05).

#### 4.5. MLKL is not phosphorylated during apoptosis in L929 cell cells

Previous research done in L929 cells revealed that MLKL was phosphorylated during SMAC mimetic induced apoptosis, which opened a possibility that p-MLKL is not an adequate marker to distinguish necroptosis from other forms of cell death<sup>39</sup>. We used WT and Optn KO L929 cells, seeded on a 12-well plate at 200 000 cells/well density. We treated cells with TNF (10 ng/ml), CHX (0.5  $\mu$ g/ml), zVAD (20  $\mu$ M) and Nec-1 (50  $\mu$ M) for 6 h, based on previous experiments where phosphorylation and degradation of MLKL reached its peak. We observed that MLKL was phosphorylated only with necroptosis treatment (TCZ) and



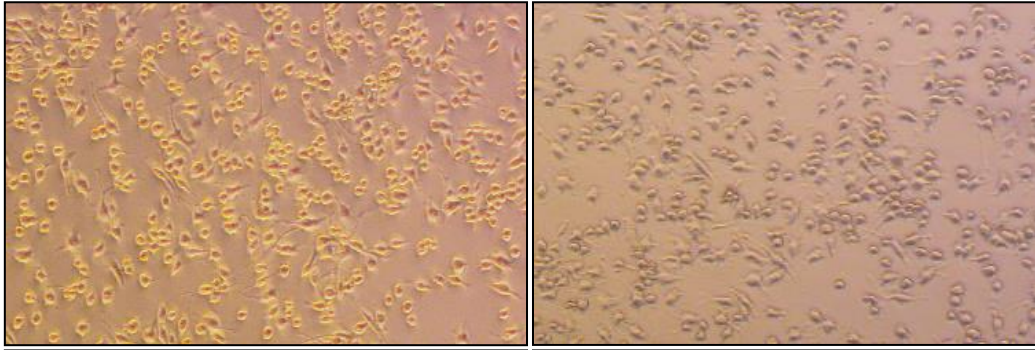
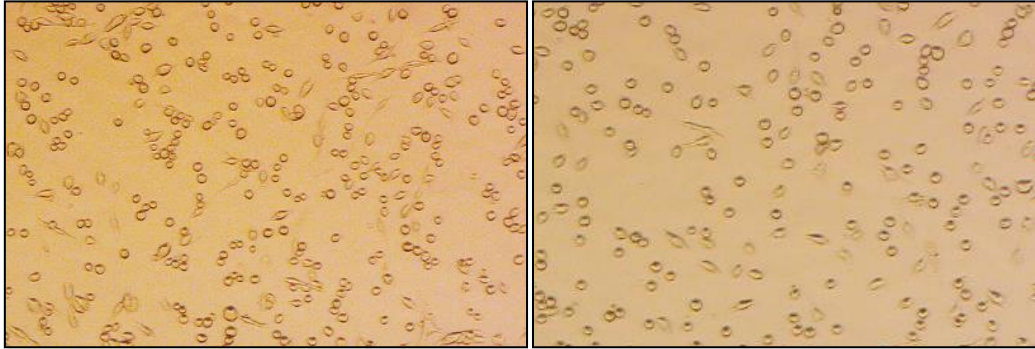
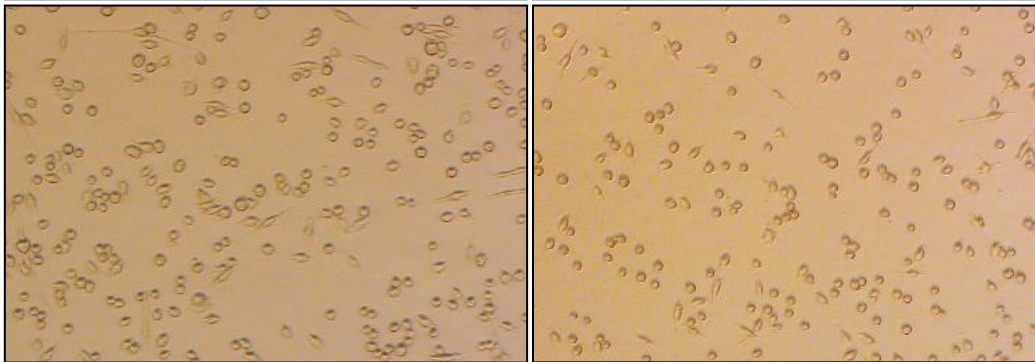
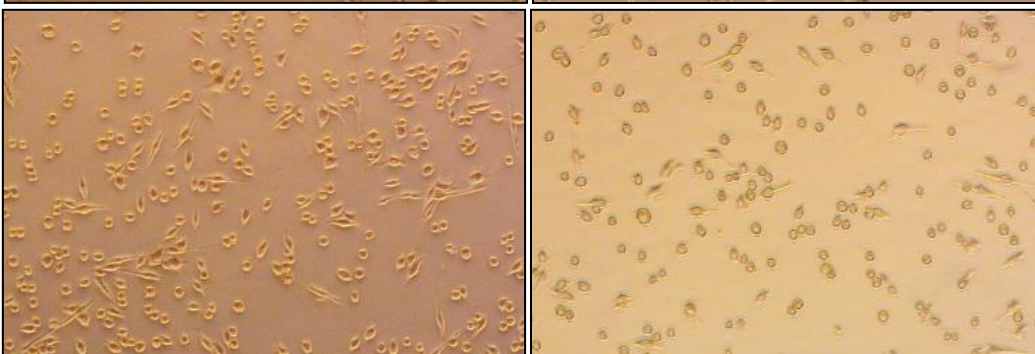
phosphorylation was inhibited with RIPK1 inhibitor (Fig. A and B). There was no specific p-MLKL band with apoptosis treatment (TC) (Fig. A and B), which confirmed that p-MLKL is present only during necroptosis. Similar to previous result, there was difference in p-MLKL levels between WT and Optn KO cells upon necroptosis treatment (Fig. B). However, it is important to note that this data is obtained from single experiment so additional experiments are necessary to confirm this conclusion.



**Figure 9. MLKL is not phosphorylated during apoptosis in L929 cell cells.** (A) L929 WT and Optn KO cells were treated with TNF (10 ng/ml), CHX (0.5 µg/ml), zVAD (20 µM) for apoptosis (TC) or necroptosis (TCZ) with addition of RIPK1 inhibitor Nec -1 (50 µM) (N) for 6h. Controls were treated with DMSO for 6h. p-MLKL was detected by immunoblotting and β-actin served as a loading control. (B) Densitometric quantification of p-MLKL after 6h treatment. The experiment was performed once so the statistical analysis could not be done.

#### **4.6. WT and Optn KO BV2 cells are not sensitive to necroptosis or apoptosis**

In order to characterize cell death in cell types predominantly involved in ALS pathogenesis, we used immortalized murine BV2 WT and Optn KO cell line and induced apoptosis and necroptosis to see if optineurin deficiency contributed to cell death. We followed the same protocol as with L929 cells and treated them with TNF (10 ng/ml) and CHX (0.5 µg/ml) to induce apoptosis, with addition of zVAD (20 µM) for necroptosis. We used a RIPK1 inhibitor Nec-1 (50 µM), as a test for efficiency of necroptosis and RIPK1-dependent apoptosis. Light microscopy images showed a reduction in cell number after treatment for apoptosis (TC) and necroptosis (TCZ) compared to control (Fig. A). After we counted live cells, we detected significant cell death compared to control. However, neither WT nor Optn KO BV2 cells were dying from necroptosis nor apoptosis since there was no increase in cell number after RIPK1 or caspase inhibition (Fig. B). Furthermore, there was no significant difference in cell death between WT and Optn KO, which means that optineurin does not sensitize cells to necroptosis in BV2 cell line. These results indicated that BV2 WT and Optn KO cells were dying from another form of death.

**A****WT****Optn KO****CTRL****TC****TC+N****TCZ****TCZ+N**

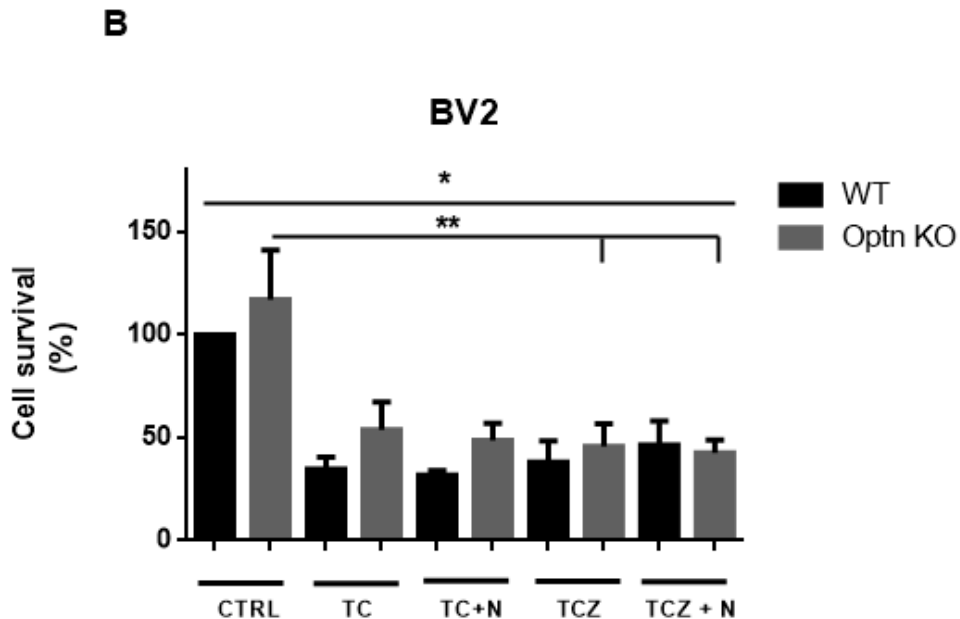


**Figure 10. WT and Optn KO BV2 cells are not sensitive to necroptosis or apoptosis.** (A) Light microscopy images of the BV2 WT and Optn KO cell lines. Cells were treated with TNF (10 ng/ml), CHX (0.5  $\mu$ g/ml), zVAD (20  $\mu$ M) for apoptosis (TC) or necroptosis (TCZ) as indicated; RIPK1 inhibitor Nec -1 (50  $\mu$ M; N) was added to block necroptosis. Control samples were treated with DMSO. (B) Live cells were counted using trypan blue exclusion assay on Neubauer hemocytometer 24 h upon treatment. Optn KO samples were normalized to WT counterparts from each experiment. Data are shown as mean  $\pm$  SEM of duplicate samples from three independent experiments (ordinary one-way ANOVA, followed by Tukey's multiple comparisons post hoc test for pair-wise comparison, \* $p$ <0.05, \*\*  $p$ <0.01).

#### 4.7. Neuro2A cells are not sensitive to necroptosis or apoptosis.

After we showed that BV2 cells are not sensitive to necroptosis, we conducted an experiment on mouse Neuro2A, in order to get better insight in neuronal death. For this experiment we treated only WT Neuro2A cells with TNF (10 ng/ml) and CHX (0.5  $\mu$ g/ml) to induce apoptosis, with addition of zVAD (20  $\mu$ M) for necroptosis. As indicated, we added Nec-1 with apoptosis and necroptosis treatment to inhibit RIPK1. Results we obtained are similar to those in BV2 cells, where there was significant cell death compared to control. However, caspase and RIPK1 inhibition did not

increase cell survival, suggesting that Neuro2A cells are also not dying from necroptosis or apoptosis (Fig.). It is important to note that our data was obtained from duplicate samples of a single experiment and without Optn KO cells, so this experiment requires repetition.

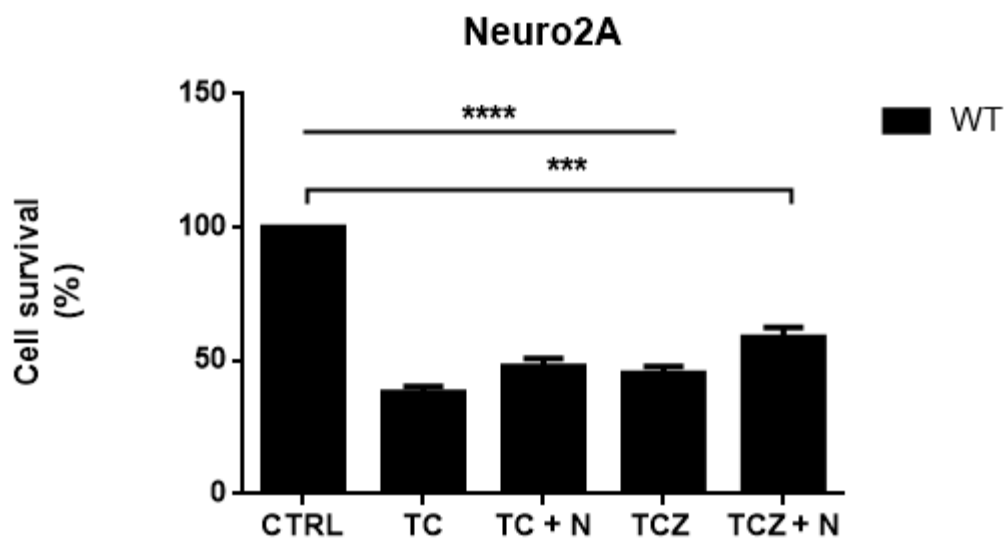


**Figure 11. Neuro2A cells are not sensitive to necroptosis or apoptosis.** Neuro2A cells were treated with TNF (10 ng/ml), CHX (0.5  $\mu$ g/ml), zVAD (20  $\mu$ M) for apoptosis (TC) or necroptosis (TCZ) with addition of RIPK1 inhibitor Nec -1 (50  $\mu$ M) (N) as indicated. Control was treated with DMSO and after 24h cell viability was measured. Data are shown as mean  $\pm$  SD of duplicate samples from one independent experiment (ordinary one-way ANOVA, followed by Tukey's multiple comparisons post hoc test for pair-wise comparison, \*\*\*  $p < 0.001$ , \*\*\*\*  $p < 0.0001$ ).

## 5. Discussion

Neuroinflammation and TNF-mediated programmed cell death are major contributors to ALS pathogenesis and neurodegeneration in general <sup>5,17</sup>. However, even now that most of the signaling events distal to TNFR1 activation have been elucidated, the molecular switch between different outcomes of the NF- $\kappa$ B pathway activation, namely RIA, RDA and necroptosis is still unclear <sup>20</sup>.

It has been suggested that ubiquitylation and phosphorylation status of RIPK1 dictate its cytotoxic potential and cell fate <sup>40</sup>. One of the possible regulators of RIPK1 activity is optineurin. In a recent study, optineurin-deficient mice exhibited ALS-like symptoms with hallmarks of necroptosis <sup>17,37</sup>. The authors also reported more proinflammatory microglia in these mice, and suggested that this is an aftermath of optineurin loss. However, the exact mechanism which optineurin regulates RIPK1 activity is still unknown. For this reason, we decided to generate a new *in vitro* model of optineurin deficiency.

A recent study has demonstrated that L929 cells with silenced optineurin were more sensitive to necroptotic death induced with mTNF or zVAD <sup>37</sup>. Silencing is more prone to artefacts than genetic models, so our first goal was to confirm that optineurin deficiency indeed sensitizes cells to necroptosis. We successfully generated Optn KO L929 stable cell line using CRISPR/Cas9 technology, which proved to be a time saving and relatively simple method for generating gene-edited cell lines. In addition, our results confirmed that WT L929 cells are indeed highly susceptible to a necroptotic stimulus. With RIPK1 inhibition, survival increased by approximately 50%, confirming that a large fraction of WT L929 cells are dying from necroptosis. We could not detect difference in cell survival between WT and Optn KO L929 cells after we induced necroptosis, suggesting that optineurin is not implicated in this form of programmed cell death.

This contrasts previously reported results in which optineurin silencing sensitized L929 cells to necroptosis, and p-MLKL levels were higher in Optn KO cells <sup>37</sup>. The reasons for this discrepancy are still unclear and could perhaps be due to an artifact of the silencing technique. Notably, in the aforementioned study, the results from cell viability tests were normalized, and no raw data of p-MLKL levels were provided. Our data showed a tendency for lower survival in Optn KO L929 cells compared to WT cells after an apoptotic trigger, and with RIPK1 inhibition there was a trend for increased survival. This could be due to the fact that optineurin binds to caspase-8 and inactivates it <sup>41</sup>, so there is a possibility that optineurin-deficient cells undergo RDA. Additional experiments, such as confirmation of caspase-3 and RIPK1 activation, are needed to confirm RDA as a potential mechanism of death. Overall, these results confirm that L929 cells are prone to necroptotic death, but optineurin loss did not significantly enhance TNF-mediated necroptosis.

Previous research showed that TNF by itself is sufficient for inducing necroptosis in L929 cell line <sup>42</sup>. Considering that there are three possible death outcomes during TNFR1 signaling, it is possible that TNF alone does not push cells necessarily toward necroptosis, but also to RIA or RDA. One study induced necroptosis in L929 cells with TNF and AZD 5582 dihydrochloride (SMAC mimetic) and generated population of cells that were positive for both p-MLKL and cleaved caspase-3 (CC3) <sup>39</sup>. This suggests that caspase inhibition prevents mixed phenotypic cell death. We showed that MLKL is not phosphorylated upon TNF and CHX treatment, and obtained a specific p-MLKL band only upon addition of zVAD. Our data confirms that TNF and CHX do not induce necroptosis, and confirm that caspase inhibition in L929 cells is required for necroptotic phenotype.

In neurodegenerative diseases, regulation of immune response is compromised and leads to chronic neuroinflammation <sup>13</sup>. Microglia is considered to be a main source of TNF, whose elevated levels can be found in the blood of ALS patients <sup>43</sup>. Primary microglia derived from Optn<sup>-</sup>

$\gamma/\gamma$  mice had elevated RIPK1 activation which was inhibited *in vivo* by Nec-1s administration and additional Ripk1<sup>D138N/D138N</sup> mutation. This mutation results in inactive kinase, and is commonly used instead of total RIPK1 knockout, since those mice die shortly after birth<sup>44</sup>. Moreover, the same microglia had elevated TNF levels that were inhibited with Nec-1s, indicating that they might be in the M1, pro-inflammatory state<sup>37</sup>.

Previous research in our lab obtained opposite results, where after LPS stimulated Optn KO BV2 cells showed no disturbance in NF- $\kappa$ B signaling, and had slightly decreased levels of TNF<sup>6</sup>. Other results in microglia generated from Optn<sup>470T</sup> mice showed no difference in TNF production upon LPS stimulation<sup>11</sup>. Data from our lab on Optn KO BV2 cells and primary microglia from Optn<sup>470T</sup> mice report normal, even lower levels of TNF compared to Optn $\gamma/\gamma$  microglia. Similar results were found in Optn $\gamma/\gamma$  BMDMs, implying that in the absence of optineurin most of the intracellular TNF is pushed to lysosomal degradation<sup>45</sup>. Thus, it is likely that optineurin regulates NF- $\kappa$ B signaling and proinflammatory cytokine production, but it is still unclear by which mechanism due to some controversial findings.

Low expression levels of MLKL were found in optineurin-deficient microglia<sup>37</sup>, indicating that microglia likely are not dying from necroptosis, although some studies suggest differently REF. However, there is no confirmation that optineurin-deficient microglia are not undergoing TNF-mediated necroptosis. Our data obtained from experiment on BV2 cell line shows that microglia were not susceptible to TNF-mediated necroptotic death. What is intriguing is that cell viability is reduced under necroptotic conditions, but it was not rescued upon RIPK1 and caspase inhibition. We could hypothesize that cells are dying in a manner different from apoptosis or necroptosis and that exogenous TNF promotes different mechanism of cell death. In addition, we should test if our microglia express any pro-inflammatory biomarkers for M1 active state and repeat cell viability using additional methods, such as MTT test or ToxiLight



assay.

Previous studies *in vitro* discovered that toxic astrocytes promote necroptotic motor neuron death. Human and mouse ESC-derived motor neurons were co-cultured with astrocytes derived from sALS patients, and their survival improved after RIPK1 inhibition <sup>46</sup>. Another recent *in vivo* study reported no improvement in motor neuron death after MLKL deletion in SOD1<sup>G93A</sup> mouse model, indicating that necroptotic pathway was not involved. They also reported no change in activation of astrocytes and microglia, and suggested that other forms of cell death are contributing to astrocyte-mediated motor neuron death in ALS <sup>47</sup>. This is in agreement with our results, where Neuro2A cells are dying after necroptosis treatment, but their viability is not improved after RIPK1 inhibition, same as BV2 cells. It is important to note that these results are obtained only in WT cells, and we cannot debate whether neurons would be dying if they are optineurin-deficient. Overall, our results suggest a possibility that additional mechanism, independent of caspase and RIPK1 kinase activity, pushes cells to death.

## 6. Conclusion

For the purpose of studying TNF-mediated programmed cell death in cells with optineurin deficiency we established Optn KO L929 fibroblast cell line using CRISPR/Cas9 method. We confirmed that L929 cells are sensitive to necroptosis. Contrary to a previous study <sup>37</sup>, we found no evidence that loss of optineurin confers higher susceptibility towards necroptosis in these cells. After conducting same experiments in microglial cell line, we did not detect any difference in survival rate between WT and Optn KO microglia. Interestingly, we observed significant cell death in both microglia and neurons, even in conditions where RIPK1 and caspases were inhibited. This was in agreement with previous studies; however, we could not determine which form of cell death is responsible for his phenotype. These results need to be confirmed in primary cells, as well as *in vivo*, since recently published papers show significant differences between *in vivo* and *in vitro* optineurin models.

## 7. References

- 1 Jung YJ, Tweedie D, Scerba MT, Greig NH. Neuroinflammation as a Factor of Neurodegenerative Disease: Thalidomide Analogs as Treatments. *Front Cell Dev Biol* 2019; **7**: 313.
- 2 Mejzini R, Flynn LL, Pitout IL, Fletcher S, Wilton SD, Akkari PA. ALS Genetics, Mechanisms, and Therapeutics: Where Are We Now? *Front Neurosci* 2019; **13**: 1310.
- 3 McCauley ME, Baloh RH. Inflammation in ALS/FTD pathogenesis. *Acta Neuropathologica* 2018. doi:10.1007/s00401-018-1933-9.
- 4 Renton AE, Chiò A, Traynor BJ. State of play in amyotrophic lateral sclerosis genetics. *Nat Neurosci* 2014; **17**: 17–23.
- 5 Markovinovic A, Cimbri R, Ljutic T, Kriz J, Rogelj B, Munitic I. Optineurin in amyotrophic lateral sclerosis: Multifunctional adaptor protein at the crossroads of different neuroprotective mechanisms. *Progress in Neurobiology* 2017; **154**: 1–20.
- 6 Rob M. Characterizing the role of optineurin in inflammatory signaling in microglial and neuronal cell lines. 2018; : 64.
- 7 Taylor JP, Brown RH, Cleveland DW. Decoding ALS: from genes to mechanism. *Nature* 2016; **539**: 197–206.
- 8 DiSabato DJ, Quan N, Godbout JP. Neuroinflammation: the devil is in the details. *J Neurochem* 2016; **139**: 136–153.
- 9 Schettters STT, Gomez-Nicola D, Garcia-Vallejo JJ, Van Kooyk Y. Neuroinflammation: Microglia and T Cells Get Ready to Tango. *Front Immunol* 2018; **8**: 1905.
- 10 Tang Y, Le W. Differential Roles of M1 and M2 Microglia in Neurodegenerative Diseases. *Mol Neurobiol* 2016; **53**: 1181–1194.
- 11 Markovinovic A, Ljutic T, Béland L-C, Munitic I. Optineurin Insufficiency Disbalances Proinflammatory and Anti-inflammatory Factors by Reducing Microglial IFN- $\beta$  Responses. *Neuroscience* (In press)
- 12 Subedi L, Lee SE, Madiha S, Gaire BP, Jin M, Yumnam S *et al.* Phytochemicals against TNF $\alpha$ -Mediated Neuroinflammatory Diseases. *IJMS* 2020; **21**: 764.
- 13 Olmos G, Lladó J. Tumor Necrosis Factor Alpha: A Link between Neuroinflammation and Excitotoxicity. *Mediators of Inflammation* 2014; **2014**: 1–12.
- 14 Rizzo FR, Musella A, De Vito F, Fresegna D, Bullitta S, Vanni V *et al.* Tumor Necrosis Factor and Interleukin-1  $\beta$  Modulate Synaptic Plasticity during Neuroinflammation. *Neural Plasticity* 2018; **2018**: 1–12.

- 15 Silke J, Rickard JA, Gerlic M. The diverse role of RIP kinases in necroptosis and inflammation. *Nat Immunol* 2015; **16**: 689–697.
- 16 Brenner D, Blaser H, Mak TW. Regulation of tumour necrosis factor signalling: live or let die. *Nat Rev Immunol* 2015; **15**: 362–374.
- 17 Yuan J, Amin P, Ofengeim D. Necroptosis and RIPK1-mediated neuroinflammation in CNS diseases. *Nat Rev Neurosci* 2019; **20**: 19–33.
- 18 Vanlangenakker N, Bertrand MJM, Bogaert P, Vandenabeele P, Vanden Berghe T. TNF-induced necroptosis in L929 cells is tightly regulated by multiple TNFR1 complex I and II members. *Cell Death Dis* 2011; **2**: e230–e230.
- 19 Amin P, Florez M, Najafov A, Pan H, Geng J, Ofengeim D *et al.* Regulation of a distinct activated RIPK1 intermediate bridging complex I and complex II in TNF $\alpha$ -mediated apoptosis. *Proc Natl Acad Sci USA* 2018; **115**: E5944–E5953.
- 20 Dondelinger Y, Jouan-Lanhouet S, Divert T, Theatre E, Bertin J, Gough PJ *et al.* NF- $\kappa$ B-Independent Role of IKK $\alpha$ /IKK $\beta$  in Preventing RIPK1 Kinase-Dependent Apoptotic and Necroptotic Cell Death during TNF Signaling. *Molecular Cell* 2015; **60**: 63–76.
- 21 D’Arcy MS. Cell death: a review of the major forms of apoptosis, necrosis and autophagy. *Cell Biol Int* 2019; **43**: 582–592.
- 22 Newton K, Manning G. Necroptosis and Inflammation. *Annu Rev Biochem* 2016; **85**: 743–763.
- 23 Xu X, Lai Y, Hua Z-C. Apoptosis and apoptotic body: disease message and therapeutic target potentials. *Bioscience Reports* 2019; **39**: BSR20180992.
- 24 Porter AG, Jänicke RU. Emerging roles of caspase-3 in apoptosis. *Cell Death Differ* 1999; **6**: 99–104.
- 25 Schneider-Poetsch T, Ju J, Eyler DE, Dang Y, Bhat S, Merrick WC *et al.* Inhibition of eukaryotic translation elongation by cycloheximide and lactimidomycin. *Nat Chem Biol* 2010; **6**: 209–217.
- 26 Degterev A, Ofengeim D, Yuan J. Targeting RIPK1 for the treatment of human diseases. *Proc Natl Acad Sci USA* 2019; **116**: 9714–9722.
- 27 Geng J, Ito Y, Shi L, Amin P, Chu J, Ouchida AT *et al.* Regulation of RIPK1 activation by TAK1-mediated phosphorylation dictates apoptosis and necroptosis. *Nature Communications* 2017; **8**. doi:10.1038/s41467-017-00406-w.
- 28 Bai L, Smith DC, Wang S. Small-molecule SMAC mimetics as new cancer therapeutics. *Pharmacology & Therapeutics* 2014; **144**: 82–95.
- 29 Yamaguchi Y, Miura M. Programmed Cell Death in Neurodevelopment. *Developmental Cell* 2015; **32**: 478–490.

- 30 Conrad M, Angeli JPF, Vandenabeele P, Stockwell BR. Regulated necrosis: disease relevance and therapeutic opportunities. *Nat Rev Drug Discov* 2016; **15**: 348–366.
- 31 Li X, Yao X, Zhu Y, Zhang H, Wang H, Ma Q *et al*. The Caspase Inhibitor Z-VAD-FMK Alleviates Endotoxic Shock via Inducing Macrophages Necroptosis and Promoting MDSCs-Mediated Inhibition of Macrophages Activation. *Front Immunol* 2019; **10**: 1824.
- 32 Beirowski B, Nógrádi A, Babetto E, Garcia-Alias G, Coleman MP. Mechanisms of Axonal Spheroid Formation in Central Nervous System Wallerian Degeneration. *J Neuropathol Exp Neurol* 2010; **69**: 455–472.
- 33 Bansal M, Swarup G, Balasubramanian D. Functional analysis of optineurin and some of its disease-associated mutants: Functional Analysis of Optineurin and its Disease-Associated Mutants. *IUBMB Life* 2015; **67**: 120–128.
- 34 Toth RP, Atkin JD. Dysfunction of Optineurin in Amyotrophic Lateral Sclerosis and Glaucoma. *Front Immunol* 2018; **9**: 1017.
- 35 Schwamborn K, Weil R, Courtois G, Whiteside ST, Israël A. Phorbol Esters and Cytokines Regulate the Expression of the NEMO-related Protein, a Molecule Involved in a NF- $\kappa$ B-independent Pathway. *J Biol Chem* 2000; **275**: 22780–22789.
- 36 Zhu G, Wu C-J, Zhao Y, Ashwell JD. Optineurin Negatively Regulates TNF $\alpha$ -Induced NF- $\kappa$ B Activation by Competing with NEMO for Ubiquitinated RIP. *Current Biology* 2007; **17**: 1438–1443.
- 37 Ito Y, Ofengeim D, Najafov A, Das S, Saberi S, Li Y *et al*. RIPK1 mediates axonal degeneration by promoting inflammation and necroptosis in ALS. *Science* 2016; **353**: 603–608.
- 38 Dermentzaki G, Politi KA, Lu L, Mishra V, Pérez-Torres EJ, Sosunov AA *et al*. Deletion of *Ripk3* Prevents Motor Neuron Death *In Vitro* but not *In Vivo*. *eNeuro* 2019; **6**: ENEURO.0308-18.2018.
- 39 Zargarian S, Shlomovitz I, Erlich Z, Hourizadeh A, Ofir-Birin Y, Croker BA *et al*. Phosphatidylserine externalization, “necroptotic bodies” release, and phagocytosis during necroptosis. *PLoS Biol* 2017; **15**: e2002711.
- 40 Delanghe T, Dondelinger Y, Bertrand MJM. RIPK1 Kinase-Dependent Death: A Symphony of Phosphorylation Events. *Trends in Cell Biology* 2020; **30**: 189–200.
- 41 Ryan TA, Tumbarello DA. Optineurin: A Coordinator of Membrane-Associated Cargo Trafficking and Autophagy. *Front Immunol* 2018; **9**: 1024.
- 42 Sawai H. Induction of Apoptosis in TNF-Treated L929 Cells in the Presence of Necrostatin-1. *IJMS* 2016; **17**: 1678.

- 43 Babu GN, Kumar A, Chandra R, Puri SK, Kalita J, Misra UK. Elevated Inflammatory Markers in a Group of Amyotrophic Lateral Sclerosis Patients from Northern India. *Neurochem Res* 2008; **33**: 1145–1149.
- 44 Polykratis A, Hermance N, Zelic M, Roderick J, Kim C, Van T-M *et al.* Cutting Edge: RIPK1 Kinase Inactive Mice Are Viable and Protected from TNF-Induced Necroptosis In Vivo. *J I* 2014; **193**: 1539–1543.
- 45 Chew TS, O’Shea NR, Sewell GW, Oehlers SH, Mulvey CM, Crosier PS *et al.* Optineurin deficiency in mice contributes to impaired cytokine secretion and neutrophil recruitment in bacteria-driven colitis. *Disease Models & Mechanisms* 2015; **8**: 817–829.
- 46 Re DB, Le Verche V, Yu C, Amoroso MW, Politi KA, Phani S *et al.* Necroptosis Drives Motor Neuron Death in Models of Both Sporadic and Familial ALS. *Neuron* 2014; **81**: 1001–1008.
- 47 Wang T, Perera ND, Chiam MDF, Cuic B, Wanniarachchillage N, Tomas D *et al.* Necroptosis is dispensable for motor neuron degeneration in a mouse model of ALS. *Cell Death Differ* 2020; **27**: 1728–1739.

## Student

## EDUCATION

- 2017 - present **Department of Biotechnology, University of Rijeka (Croatia)**  
Graduate program **Biotechnology in Medicine**  
Grade point average 4.43 (max 5.00)
- Jun 2019  
Summer school **Pathophysiology and Current Public Health Issues** (Rijeka, Croatia)  
St. Cloud State University/University of Rijeka
- 2014 - 2017  
Bachelor of **Biotechnology and Drug Research** (Magna cum laude)  
**Department of Biotechnology, University of Rijeka (Croatia)**  
Undergraduate program **Biotechnology and Drug Research**  
Grade point average 4.58 (max 5.00)
- 2010 - 2014 **High school Isidora Kršnjavoga Našice (Croatia)**

## EXPERIENCE

- Feb – May 2020 **Erasmus + practice**, University of Ulm,  
Neurology Department (Germany), supervisor:  
Prof. Jochen Weishaupt
- Feb – Aug 2019 **Master thesis researcher**  
Department of Biotechnology, University of Rijeka (Croatia)  
Laboratory of molecular immunology; mentor: dr.sc. Ivana Munitić  
Master thesis: **In vitro characterization of TNF-mediated programmed death in cells with optineurin deficiency**
- Feb - Jul 2017 **Bachelor thesis researcher**  
Department of Biotechnology, University of Rijeka (Croatia)  
Laboratory of organic chemistry  
Bachelor thesis: **Synthesis of thieno [2,3-d] oxepin derivative as a precursor for further development of molecules with potential anti-inflammatory effect**
- 29/05/2017 –  
09/06/2017 **Student practice at JGL.d.d, Research and development**  
-Fotochemistry
- Mar – May 2016 **Volunteering at laboratory of organic chemistry**  
-Synthesis of coumarin compounds

## CONTACTS

## Email:

[karla.dubaic@gmail.com](mailto:karla.dubaic@gmail.com)

Phone: +385911544713

Address: Mugarička 15, 51  
000, Rijeka

## JOB RELATED SKILLS

- Western blot
- PCR
- Cell culture
- Tissue preparation
- Spectrophotometry
- Liquid chromatography
- Image J
- GraphPad Prism 6
- MS Office
- Chimera
- PyMOL
- Tenua
- Avogadro – Gamess
- VMD-NAMD

## LANGUAGES

Croatian (mother tongue)

**English (C1)** – OLS  
evaluation

## MEMBERSHIPS

Member of the Student  
Association of Biotechnology of  
Rijeka (USBri)